IMAGE & SIGNAL PROCESSING

Age Prediction Based on Brain MRI Image: A Survey

Hedieh Sajedi [1,2] · Nastaran Pardakhti [1]

Abstract

Human age prediction is an interesting and applicable issue in different fields. It can be based on various criteria such as face image, DNA methylation, chest plate radiographs, knee radiographs, dental images and etc. Most of the age prediction researches have mainly been based on images. Since the image processing and Machine Learning (ML) techniques have grown up, the investigations were led to use them in age prediction problem. The implementations would be used in different fields, especially in medical applications. Brain Age Estimation (BAE) has attracted more attention in recent years and it would be so helpful in early diagnosis of some neurodegenerative diseases such as Alzheimer, Parkinson, Huntington, etc. BAE is performed on Magnetic Resonance Imaging (MRI) images to compute the brain ages. Studies based on brain MRI shows that there is a relation between accelerated aging and accelerated brain atrophy. This refers to the effects of neurodegenerative diseases on brain structure while making the whole of it older. This paper reviews and summarizes the main approaches for age prediction based on brain MRI images including preprocessing methods, useful tools used in different research works and the estimation algorithms. We categorize the BAE methods based on two factors, first the way of processing MRI images, which includes pixel-based, surface-based, or voxel-based methods and second, the generation of ML algorithms that includes traditional or Deep Learning (DL) methods. The modern techniques as DL methods help MRI based age prediction to get results that are more accurate. In recent years, more precise and statistical ML approaches have been utilized with the help of related tools for simplifying computations and getting accurate results. Pros and cons of each research and the challenges in each work are expressed and some guidelines and deliberations for future research are suggested.

Keywords Age prediction · Brain MRI · Brain age · BAE · Chronological age · Deep Learning · Image processing · Machine Learning

Introduction

Human age estimation is the task of training a ML system based on an input dataset to predict the chronological age. Chronological age of a person is assumed from his/her date of birth, which is obtained from the birth records. It is

✉ Hedieh Sajedi
hhsajedi@ut.ac.ir

Nastaran Pardakhti
n.pardakhti@ut.ac.ir

[1] School of Mathematics, Statistics and Computer Science, College of Science, University of Tehran, Tehran, Iran

[2] School of Computer Science, Institute for Research in Fundamental Science (IPM), P.O. Box 19395-5746, Tehran, Iran

calculated by subtracting the birth date from the date on which physical records of his/her are exposed. It is a challenging task in computer vision and image processing and can be based on various mediums such as the following:

- **Facial image**: Predicting age by face images is widely investigated by utilizing the whole skin area in image particularly the skin around the eyes, mouth, forehead, etc. It means to specify skin specificities such as wrinkle features, skin color, and other objects of face, which have changes through aging [1, 2]. Various ML techniques including shallow classification methods and DL methods have been used in this area, and accurate results were reached [3–5] (e.g. Mean Absolute Error (MAE) = 3.31 on Morph II dataset). The framework of deep Convolutional Neural Networks (CNN) is one of the main DL methods used for the image classification tasks. In [4], a group-aware formulation for CNN network is presented which is based on using the raw pixels of face images. The

importance of some CNN factors such as its depth, loss function, and training approach are evaluated to get the best result of age prediction and gender recognition [3].

- **DNA methylation**: DNA methylation is one of the mediums, which can be used for age estimation. In [6], the validity of age estimation based on DNA methylation, which has been proposed in [7], is evaluated. The study of DNA methylation changes in particular Guanine residues (CpG) sites (DNA methylation mostly occurs on Cytosines followed by CpG [8]), might be useful in age estimation task. The age estimation for whole blood based on Massive Parallel Sequencing (MPS) is performed using Random Forest (RF) algorithm [9]. In the crime investigation fields, the age estimation by DNA profiles would be so helpful since it makes further information about profiles do not exist in the criminal database of DNA. In [10], the relation between signal joint T cell receptor excision circle (sjTREC) quantity and age is established to add predicted age to the DNA achieved factors.

- **Various skeleton bones in body**: There are various skeletal bones of human body, which might be visualized and used for age estimation issues. Chest plate radiography [11], knee skeleton [10], hand skeleton [12, 13], medial epiphysis of the clavicle [14–17], cervical vertebra [18], temporal bone [19], mandibular ramus [20], teeth development [21–24], the apophysis of the iliac crest [25–27], the ischial tuberosity [28–30] and so on are different skeletal images which have been used for age prediction.

Some investigations have been based on dental issues for the purpose of human age prediction. Ge et al. showed the relationship between pulp chamber volume of first molars and age and proposed a mathematical model based on pulp chamber volume to predict age [21]. In the area of chest plate radiographies, Costal cartilage ossification on chest plate radiographs is a useful method for age prediction [11]. Monum et al. proposed a mathematical formula to calculate age in such a way that eight features were selected and scored, causing composite score and used the composite score in formula to calculate age.

- **Brain MRI**: MRI data analysis can be used to predict a person's age. Most, but not all, individuals' brain-derived estimated age is close to their chronological age [31]. Age estimation based on imaging datasets of brain requires strong knowledge about image processing and computer vision, and it is necessarily needed to know about the suitable classification and regression techniques to get perfect results in predicting the physical age by brain MRI.

Cerebrum, the largest part of the brain, can be divided into six lobes: frontal, temporal, parietal, limbic, occipital, and insula. The cortical thickness decline is shown to be variable among people in each cortex lobe [32]. The approaches of analyzing cortical thickness based on MRI images can be generally classified into two main groups of surface based and voxel based [33].

It has been shown that the brain structure changes over the natural aging process or a neurodegenerative disease [34–38]. Some demographic features such as gender, education, etc., are shown to be effective in brain aging. In [36], the Gray Matter Ratio (GMR) is calculated and it is shown that the age, gender, and body mass index have effects on GMR. The consequences would be used in differentiating the brain aging caused by normal aging or caused by a neurodegenerative disease. Also, there are relationships between education, physical activity, and some positive acts like meditation on brain morphology to get younger, as some accelerated aging processes such as Alzheimer Diseases (AD) make brain morphology older [39, 40]. By comparison of the brain age with the chronological age, it is possible to understand weather a human has such a disease or to early detection of diseases [41].

In 2010, Washington University researchers working with resting-state fMRI data from 238 individuals between 7 and 30 years of age showed that the strength of correlated activity between brain regions is a good indicator of an individual's age [42]. Their Support Vector Machine (SVM)-based multivariate pattern analysis method allowed them to predict 55% of the variance in age within this cohort. In another research, Brown et al. [43] use measures of brain anatomy rather than brain activation to predict age. Their analyses are based on multi-modal structural MRI data from a diverse sample of 885 typically developing individuals, collected from 12 MRI scanners at nine institutions across the USA.[1]

The human aging process causes some changes in the structure of brain and cerebral cortex during the lifetime. The hopeful aspect is that it is possible to predict the accurate chronological age of healthy individuals usually by T1-weighted MRI using ML techniques. It has been shown that neurodegenerative diseases cause the brain structure to get older, and this is the most interest of using ML techniques to predict age and diseases such as Alzheimer, Schizophrenia, and Diabetes. To analyze different algorithms on various datasets, there may be some preprocessing methods to reduce negligible features, or no preprocessing methods may be used such as what is done in deep learning approach, which offers a compressed representation of large datasets [44].

In addition to the traditional classification and image processing methods, there is an idea of the modeling the human brain neurons tasks computationally to train Artificial Neural Networks (ANN). In the recent years, ANN and DL methods have become so popular and are widely used in the various classification tasks.

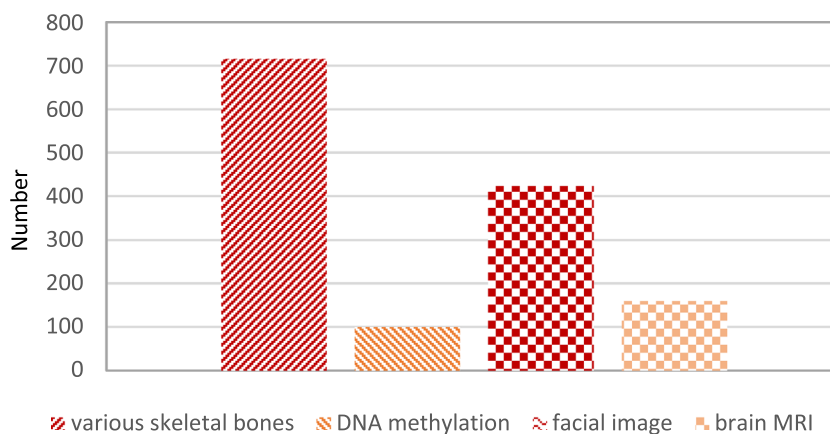[1] http://chd.ucsd.edu/research/ping-study.html

The brain age prediction is useful in offering clinically biomarkers and early detection of neurodegenerative diseases. The studies have been on various brain datasets of structural or functional data, while Liem et al. use multimodal brain imaging data to improve BAE and showed that in this way, the MAE would decrease [45]. Multimodal brain imaging biomarkers are more suitable techniques utilized for predictions based on brain images. The prediction of explicit values is done using the information of several modalities and the effect of using that, is showed to be useful in clinical decisions [46].

The paper leads the reader through several used BAE techniques, as well as applications thereof. The goal of this paper is to both, introduce the rich literature in this area, as well as equip the reader with the tools and techniques needed to analyze MRI images and learn from them.

In this paper, the below questions are answered, while leaving them open.

Q1:   Is there any way to calculate brain age by brain MRI images?

Q2:   Do neurodegenerative diseases cause changes in brain structure?

Q3:   Is it possible to specify the chronological age by brain age?

Q4:   What is a suitable approach for MRI based age prediction?

Q5:   What are the requirements of such a system to predict brain age?

Q6:   Which systems are more accurate? Pixel-based, voxel-based or surface-based?

Q7:   Is spatial normalization, resampling, and spatial smoothing, a necessary step in preprocessing?

Q8:   Among Gray matter (GM), White Matter (WM) and Cerebrospinal Fluid (CSF), which is more significant in age prediction?

Q9:   In voxel-based systems, is the voxel size effective in age prediction?

Q10:   Instead of using GM and WM, can we use smaller parts of the brain for BAE?

Q11:   Are atlas-based methods useful in BAE?

Q12:   What is the best result so far has been achieved for BAE?

Q13:   What is the convenient size of training data for BAE?

Q14:   What are challenges and solutions in brain age prediction?

Q15:   What can brain MRI imaging produced as quantitative and qualitative descriptions for predicting age?

The organization of the paper is as the following. Section 2 describes the research methodology and Section 3 is about MRI images. Section 4 is about image processing and summarizes preprocessing methods of MRI images and available preprocessing tools. Prediction systems, which are categorized into two major classes, are described in Section 5. Section 6 is about our implementation. Discussion is presented in Section 7 and Section 8 concludes the paper.

Research methodology

All searches for research papers and reports have been done based on search on ScienceDirect, IEEE, Scopus, and PubMed in all years to March 2018. In the area of age estimation based on various mediums except brain MRI, more than 1200 papers are found with the following keywords:

– age AND (estimation OR prediction) AND (radiograph OR radiography OR radiographic)
– age AND (estimation OR prediction) AND ray
– age AND (estimation OR prediction) AND skeletal
– age AND (estimation OR prediction) AND bone
– age AND (estimation OR prediction) AND DNA
– age AND (estimation OR prediction) AND face
– age AND (estimation OR prediction) AND facial

Figure 1 illustrates the variation of published age prediction studies based on different mediums until November 2018. The diagram is based on the number of published papers using above-mentioned keywords.

Fig. 1 Comparison of the number of papers in age estimation based on various mediums

In the area of brain MRI based age estimation, about 160 papers were found at the first step with the keywords:

- Age AND (estimation OR prediction) AND MRI
- Age AND (estimation OR prediction) AND brain
- BrainAGE

At the second step, more than 80 papers found manually related to brain age estimation. Finally, the duplicated results are eliminated and about 40 papers are selected as brain age estimation studies. The searches are only limited to document title. Key aspects of each study such as dataset, location of study, type of learning method, preprocessing method, and the best-achieved results are provided in different tables. Figure 2 compares the number of BAE studies in different libraries.

Figure 3 shows the publishing trends by plotting the quantity of publications from 1999 to 2018. A relatively stable growth in the number of publications can be observed after 2011. Some downward trend in the 2011/2014/2016 were made up immediately by a sharp rise in the number of publications. This trend suggests brain age estimation hitherto remains a valuable research topic.

MRI

There are some medical imaging tools for capturing the image of the body organs such as MRI, functional MRI (fMRI), Diffusion Tensor Imaging (DTI), Positron Emission Tomography (PET), Electroencephalography (EEG) and Magnetoencephalography (MEG) [47]. Among these medical tools, MRI is the most popular technique for its advantages in biomedical analysis, perfect diagnosis, and high performance especially in the cerebrum [48–50]. MRI devices utilize strong magnets and radio waves to capture the body organs in a way that the whole tissue of organ containing anomaly tissues

would be shown [51–53]. MRI images contain a great amount of information [49]. It has the potency to visualize the organ in three planes, axial, sagittal, and coronal. Figure 4 illustrates three anatomical planes extracted from the OASIS database, which is a MRI brain image database.

To visualize the body tissues, MRI uses the water molecules of the examined tissue and the magnetization properties of its nucleus. It generates a powerful magnetic field to force the protons of the water nucleus to align with that field. Next, the scanner produces a radiofrequency energy to perturb the magnetization field. This process causes the protons to motivate, spin out, and exhaust the magnetic field. When the radiofrequency energy is turned off, the protons return to their normal spin, the energy released and the time of realignment could be computed. To transform the signals to corresponding intensity levels, Fourier transformation is used which causes to produce an image matrix. The pulses of radiofrequency sequence may be different so different kinds of images are generated. Repetition Time (TR) is the total time between consecutive radiofrequency pulse sequences, which are exerted to the same slice. Time to Echo (TE) is the time between the delivery of the radiofrequency pulse and the echo signal received later. There are two different relaxation times, T1 and T2. T1, also known as longitudinal relaxation time, is the required time for motivated protons to return to their normal spin. T2, also called transverse relaxation time, is the required time for motivated protons to return to their normal spin or go out of phase with each other. Various kinds of tissues have various T1 and T2 [54–56]. Figure 5 illustrates samples of T1 and T2 images.

T1 and T2 are two templates for capturing MRI images. Talairach and Tournoux in Montreal Neurological Institute (MNI) of McGill University Health Centre developed a 3D coordinate system for stereotactic localization in Neurosurgery. An improved version was later made called the MNI152 (averaged sort of) scans were used to locate
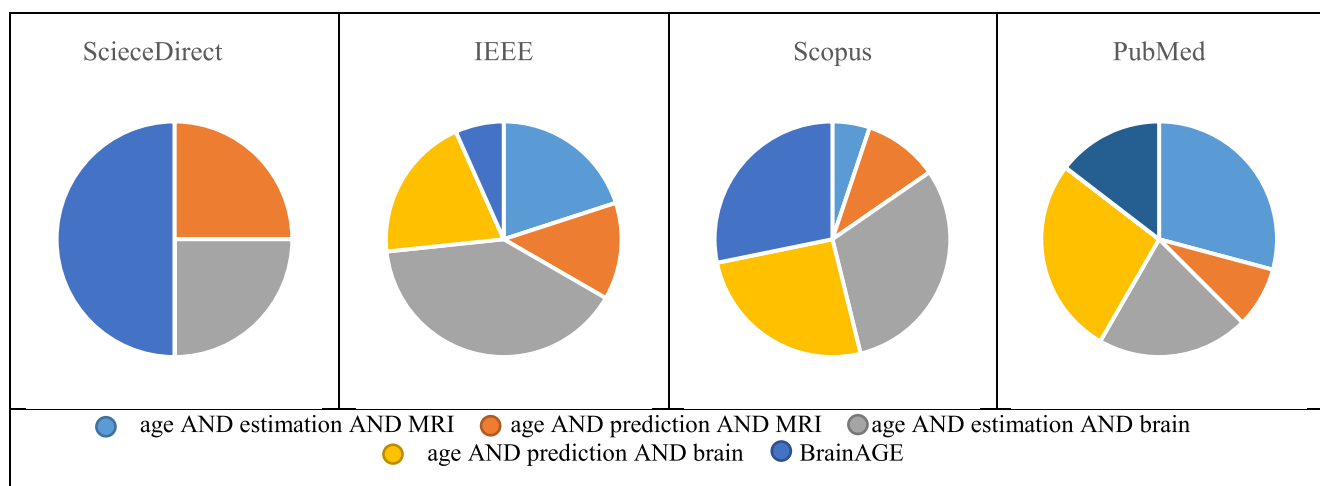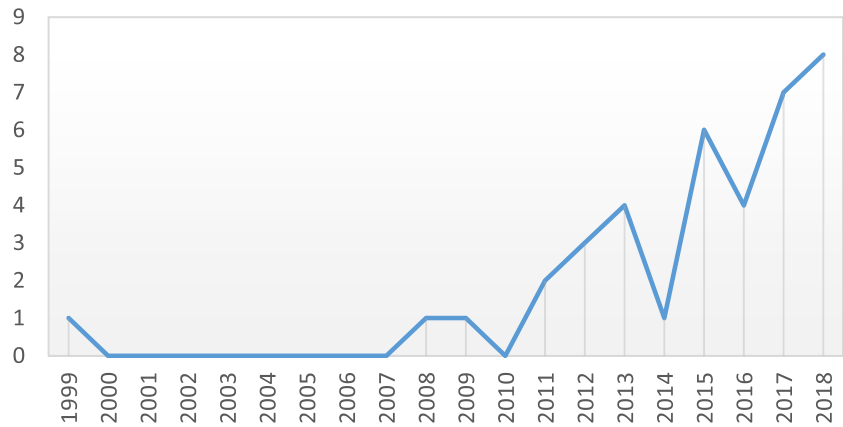

Fig. 2 Comparison the results of four library databases at the second step

Fig. 3 BAE publishing trends

structures. To perform group studies using functional imaging data, the individual brain images are usually transformed into a common coordinate space. The two most widely used spaces in the neuroscience community are MNI152 and ICBM152, which are templates for analyzing groups of MRI images [57].

Computational researches on MRI have been on various fields, such as diagnosis of different kinds of cancers [58–60]. MRI based age prediction is often done using structural T1-weighted images. The most frequently repositories of brain images are introduced in Tables 1 and 2 is about details of datasets used in various researches.

MRI file formats

Medical images like MRI, CT, and etc., may be saved in different file formats. In this section, some of the most important medical file formats like Analyze, Neuroimaging Informatics Technology Initiative (NIfTI), DICOM, and Minc are discussed briefly. Also, there are two main groups of medical imaging formats. The formats such as DICOM, which are created to standardize the images produced by imaging modalities, and the formats like Analyze, NIfTI, and Minc which are created to simplify the post-processing acts [70]. Table 3 summarizes these formats clearly and in the following, we briefly describe the mentioned formats.

Analyze Analyze 7.5 was the first format designed with the capability of storing the data in multidimensional (3D and 4D[2] data) form. The Analyze file format includes two binary files to represent the raw image data in .img extension and the metadata in .hdr extension separately. The size of the header is 348 bytes, which is prepared in C programming language and needs special software to read and edit. Analyze is categorized as an old file format. One of the restrictions of using it is that it does not support the certain data types. In addition, it does not store enough information about the image.

Minc The Minc file format was released to present a flexible format to deal with several formats from different scanners. The first version, Minc1, was based on Network Common Data Format (NetCDF) data format. Because of the problems happening due to large data files, the data format was changed to Hierarchical Data Format version 5 (HDF5) which is called Minc2.
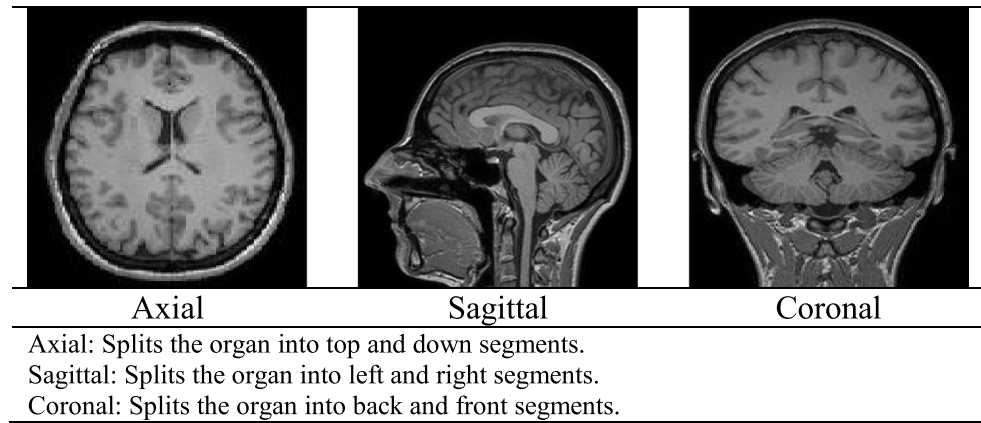
DICOM This medical imaging standard is the backbone of all medical imaging departments. Although it is born in 1993, the actual introduction happens at the end of 1990s. The construction of DICOM has been based on the fact that the image pixel data without its metadata has not the full meaning of a medical image. So, the image data and the metadata are combined together in a single file. In addition, the header may have different sizes because of the nature of the information saved in it. It includes image matrix information, the procedure of creating the images, and some personal information about the patients.

NIfTI This format was created at the beginning of the 2000 to keep the utilities of the Analyze, while eliminating the weaknesses. NIfTI format has the ability to save the image orientation in header and it allows the data type unsigned 16-bit to be stored, which was not supported in Analyze. The images are usually saved in a unique .nii file instead of being saved in the form of header and image data separately. An .nii file has 352 bytes. Four bytes are extra bytes to create a multiple of 16 size and to allow the storage of extra metadata.

Image processing

In this section, MRI image preprocessing, dimensionality reduction, and segmentation of brain images for the age estimation task are reviewed.

---

[2] It is usually about the temporal information.

Fig. 4 Samples of brain image in different planes

| Axial | Sagittal | Coronal |

Axial: Splits the organ into top and down segments.
Sagittal: Splits the organ into left and right segments.
Coronal: Splits the organ into back and front segments.

MRI image Preprocessing

Image preprocessing refers to the important processes should be done on raw images or the images at lowermost level of abstraction to prepare them for additional analysis. Preprocessing causes the images to highlight the important details and eliminate the distortions. Some operations such as rotation, scaling, etc. are categorized as preprocessing [71]. Other operations such as illumination corrections, morphology, segmentation, edge enhancements, etc. are discussed in [72] according to the different vision pipelines.

Usually, MRI images used for classification and segmentation are images obtained from scan centers or publicly available databases. These are raw images generally consist of several unreal parts such as intensity inhomogeneity, extra cranial tissues, etc. and have various types of noise. Since using raw images is not suitable and reduces the overall accuracy, appropriate techniques of preprocessing and feature extraction are definitely needed to improve the images quality [73]. There are many investigations in the area of decreasing such unreal parts of MRI images [74–76]. MRI image preprocessing is a necessary part in MR image processing contained different processes to improve image quality or to standardize its geometric and intensity patterns [77]. The preprocessing of brain images is often included spatial normalization, resampling, and spatial smoothing to meet some necessities including same space for all scans and same voxel size [62, 78, 79].

Normalization and reslicing

The subjects typically have head motion during the scan procedure and this causes some within scanner variability. To deal with this problem, a method known as resampling is used. Resampling is about a transformation, which reduces the variations between the following scans and a reference scan.

In addition, there are morphometric variations among the subject brains. The structure of brain is different among people and this is the reason of necessity of a normalization step. In the normalization step, a normalization function is applied to map all the scans to a template scan.

Fig. 5 Samples of brain T1 and T2 weighted images

T1 Weighted   T2 Weighted
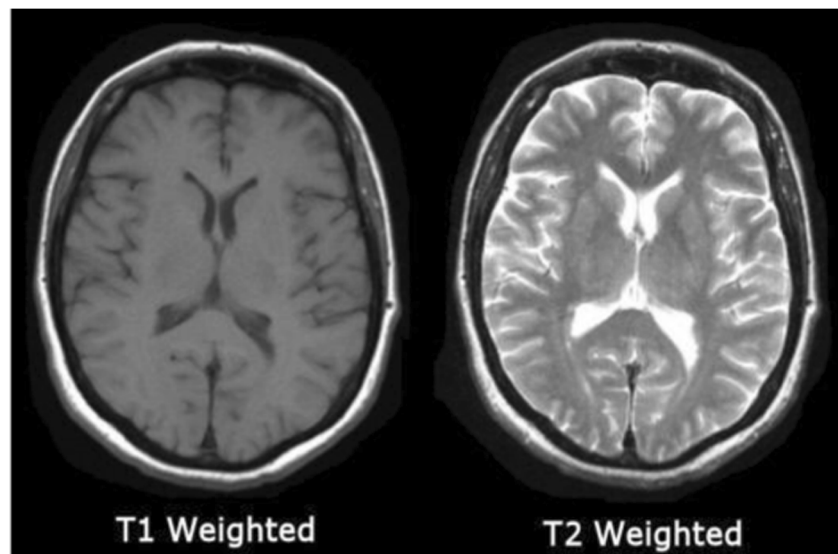
Dependent on the parameters of MRI devices, the number of slices, and the properties of images are different. Furthermore, based on the location of head of the person whose brain is scanning, the border around the brain images may be different compared to other MRI scanning. To make scanned images of different person with the similar size of borders, normalization is used to make the border of scanned images the same. Figure 6 shows a sample brain MRI before and after normalization.

Even when the devices and the parameters are the same, two slices with the same number in MRI of two persons, may not be the images from the same level of the two brains. In this case, reslicing is employed to adjust the images in similar level of the brains.

After the resampling and the normalization steps, a convolution step is commonly done due to reduce the noise. For example, a Gaussian kernel is utilized to convolve the images in [78].

Figure 7 show the levels of brain scanning in MRI in (a), some samples of scanned images are shown in (b) and the number of images (N) depends on the preset parameters of device. Two brain images with the same number in MRI image sets and different levels of brain are displayed in (c).

Lancaster et al. proposed a ML based age prediction approach in such a way that resampling parameters are learned by Bayesian optimization instead of choosing randomly [62]. In addition, they reported that the optimized voxel size and smoothing kernel size are 3.73, 3.68, respectively.

MRI preprocessing tools

In the area of brain age estimation, the researches and analyses are more challenging compared to other problems, because of the small interclass changes between different age classes. In this area, preprocessing of the input images is very important and interesting. The input images should be preprocessed properly to get ready for training a ML system with uniform and suitable input data.

The primary goal of Neuroimaging Informatics Technology Initiative[3] is to provide coordinated and targeted service, training, and research to speed the development and enhance the utility of informatics tools related to neuroimaging. The National Institute of Mental Health and the National Institute of Neurological Disorders and Stroke are joint sponsors of this initiative.

Some brain image preprocessing tools are available which are listed in Table 4 and described in the following.

Statistical parametric mapping (SPM) SPM is the mostly used preprocessing toolbox for neuroimaging data used by recent investigations (Table 5). It is a brain image analysis toolbox,

---

[3] http://nifti.nimh.nih.gov/nifti-1/

Table 1 List of public database & repositories

database	Repository details (URL address)	No. of samples	Age range	Scanner (Field strength)	Scan
IXI (Information eXtraction from Images)	http://biomedic.doc.ic.ac.uk/brain-development	561	20-86	Philips Intera (3 T); Philips Gyroscan Intera (1.5 T); GE Signa (1.5 T)	T1-FFE; MPRAGE
OASIS = The Open Access Series of Imaging Studies	http://www.oasis-brains.org	288	18-90	Siemens Vision (1.5 T)	MPRAGE
Beijing Normal University	INDI (International Neuroimaging Data-sharing Initiative) http://fcon_1000.projects.nitrc.org	181	16-28	Siemens (3 T)	MPRAGE
MCIC (MIND Clinical Imaging Consortium)	COINS (Collaborative Informatics and Neuroimaging Suite) http://coins.mrn.org	93	18-60	Siemens Sonata/Trio (1.5/3 T); GE Signa (1.5 T)	MPRAGE; SPGR
ICBM (International Consortium for Brain Mapping)	LONI IDA (Laboratory of Neuro Imaging Image & Data Archive) https://ida.loni.usc.edu	322	24-60	Siemens Magnetom (1.5 T)	MPRAGE
MIRIAD (Minimal Interval Resonance Imaging in Alzheimer's Disease)	UCL Dementia Research Centre https://www.ucl.ac.uk/drc/research/miriad-scan-database	23	58-85	GE Signa (1.5 T)	3D IR-FSPGR
CADDementia = Computer-aided diagnosis of Dementia	http://caddementia.grand-challenge.org	12	55-79	GE Signa (3 T)	3D IR-FSPGR

Table 2   Summary of datasets used in MRI based age prediction researches

Ref.	Dataset Name or Description	No. of samples	Age Range Mean± Standard Deviation (SD)	No. of subject gender Male/Female
[44]	BANC [a]-Obtained from 14 public sources	2001 healthy images Train: 1601 Validation: 200 Test: 200	Range: 18-90 36.95 ± 18.12	1016/985
[61]	Obtained from 8 public sources [b]	Train: 1537 healthy	Range: 18-90 41.82 ± 20.01	768/769
		Validation: 113 healthy	43.3 ± 20.24	49/64
		Test: 99 TBI patient	37.98 ± 12.43	72/27
[62]	BAHC [c]	Train: 2003 healthy	Range: 16-90 36.50 ± 18.52	1016/987
		Validation: 648	Range: 18-88 54.28 ± 18.56	324/324
[63]	Obtained from 14 public sources	Train: 2001 (Validation: 10-fold)	Range: 18-90 36.95 ± 18.12	1016/985
		Test: 669	72.67 ± 0.73	352/317
[35]	RSS [d]	988 healthy images Train: 888 Validation: 100	Mean: 63.3 ± 13.0	433/555
	ADNI	509 images Train: RSS988 Test: 299	–	270/239
[36]	part of the Aoba Brain Imaging Project	381 images	Range: 28-89 M: 60.0 ± 11.6 F: 57.6 ± 12.0	158/223
[37]	A part of MAAS [e] study	37 cognitive Decliners	Range: 53-84 72.5 ± 7.9	19/18
		38 non- Decliners	Range: 52-82 71.8 ± 7.7	18/20
[41]	Provided by Aoba brain image research center and Sendai Tsurugaya project	Train: 600 Validation: 499	Range: 20-80	–
[64]	ICBM [f]	84 healthy images	Range(M): 19-73 M: 44.7 ± 15.4 Range(F): 19-79 F: 43.3 ± 19.3	41/43
[40]	Self-collected	331 images	Range: 19-79	149/182
[39]	Self-collected	Train: >650	Range: 19-86	–
		Control: 50	Range: 24-77 51.4 ± 11.8	28/22
		Meditation: 50	Range: 24-77 51.4 ± 12.8	28/22
[65]	IXI [g] + [66]	Train: 655 healthy	Range: 19-86	310/345
	ADNI	Test: 334	Range: 55-90	166/168
[38]	ABSIS [h]	20 healthy images (Leave-one-out method)	Range: 50-86	–
[45]	LIFE [i] [67]	2354 images Train: 1177 Evaluation: 117	Range: 19-82 58.68 ± 15.17	1234/1120
	NKI [68]	475 images	–	–
[69]	Self-collected	112 images	Range: 50-79 67.5 ± 7.2	54/58
[32]	Self-collected [j]	Before noise removal: 2911	Range: 45-91	1460/1451
		After noise removal: 2705	64.2 ± 7.1	1368/1337

[a] (Brain-Age Normative Control): 184 ABIDE (Autism Brain Imaging Data Exchange), 179 Beijing Normal University, 49 Berlin School of Brain & Mind, 12 CADDementia, 31 Cleveland Clinic, 322 ICBM (International Consortium for Brain Mapping), 561 IXI (Information eXtraction from Images), 93 MCIC (MIND Clinical Imaging Consortium), 23 MIRIAD (Minimal Interval Resonance Imaging in Alzheimer's Disease), 39 NEO2012 (Adelstein, 2011), 160 Nathan Kline Institute (NKI) / Rockland sample, 288 OASIS, 24 WUSL (Power, 2012), 36 TRAIN-39

[b] 184 ABIDE, 82 ADNI (Alzheimer Disease Neuroimaging Initiative), 179 Beijing Normal University, 49 Berlin School of Brain & Mind, 31 Cleveland Clinic, 561 IXI, 160 NKI / Rockland sample, 291 OASIS

[c] (Brain-Age Healthy Control): 184 ABIDE, 181 Beijing Normal University, 49 Berlin School of Brain & Mind, 12 CADDementia, 31 Cleveland Clinic, 322 ICBM, 561 IXI, 93 MCIC, 23 MIRIAD, 39 NEO2012 (Adelstein, 2011), 160 NKI / Rockland sample, 288 OASIS, 24 WUSL (Power, 2012), 36 TRAIN-39

[d] 988 Rotterdam Scan Study (RSS)

[e] Maastricht Aging Study (MAAS)

[f] International Consortium of Brain Mapping (ICBM) dataset at Montreal Neurological Institute (MNI)

[g] http://fantail.doc.ic.ac.uk

[h] http://www.oasis-brains.org

[i] http://life.uni-leipzig.de

[j] The Health Promotion Center of Samsung Medical Center (SMC), Seoul, Korea

Table 3   The summery of medical file formats properties [70]

| Format	Date of birth	Header	Extension	Data types
Analyze	end of 1980s	Fixed-length: 348 byte binary format	.img and .hdr	Unsigned integer (8-bit), signed integer (16-, 32-bit), float (32-, 64-bit), complex (64-bit)
Minc	1992	Extensible binary format	.mnc	Signed (from 8- to 32-bit), unsigned integer (from 8- to 32-bit), float (32-, 64-bit), complex (32-, 64-bit)
DICOM	1993	Variable length binary format	.dcm	Signed (from 8- to 32-bit*), unsigned integer (from 8- to 32-bit*), float not supported
NIfTI	beginning of 2000s	Fixed-length: 352 byte binary format (348 byte in the case of data stored as .img and .hdr)	.nii	Signed (from 8- to 64-bit), unsigned integer (from 8- to 64-bit), Float (from 32- to 128-bit), complex (from 64- to 256-bit)

* 32-bit only allowed for radiotherapy dose

which segments the image into GM, WM, and CSF. It is a voxel-based method refers to the construction and assessment of spatially extended statistical processes used to test hypotheses about functional imaging data [79]. SPM finds particular properties of the brain image data in a specific region by generating statistical models, giving a statistical significance map of the considered regions. It maps all the scans to a unique template space to reduce the anatomical differences of the various subjects and to get the valid comparison results [78].

The software is implemented by the main theories of SPM in MATLAB programming language and is freely available to display images, DICOM import, or to do some preprocessing issues such as segmentation, smoothing, etc. Figure 8 shows the segmentation outputs of it. The recent version published is SPM12.

The brain imaging data sequences processed by SPM can be a set of various images, or time-series from the same subject. The current release is designed for the analysis of Functional MRI (fMRI), positron emission tomography (PET), Single-photon emission computed tomography (SPECT), Electroencephalography (EEG) and Magnetoencephalography (MEG) [79].

The Diffeomorphic Anatomical Registration Through Exponentiated Lie algebra (DARTEL) is a diffeomorphic image registration algorithm. Image registration is to map one
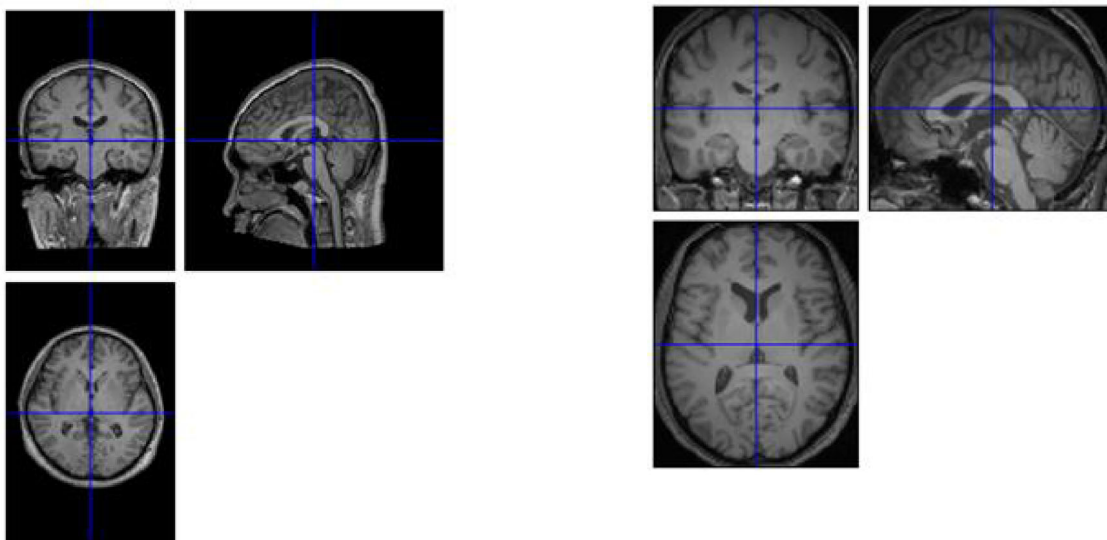
A sample MRI image before normalization	After normalization of (a)

Fig. 6 A sample of brain MRI **a** before and **b** after normalization
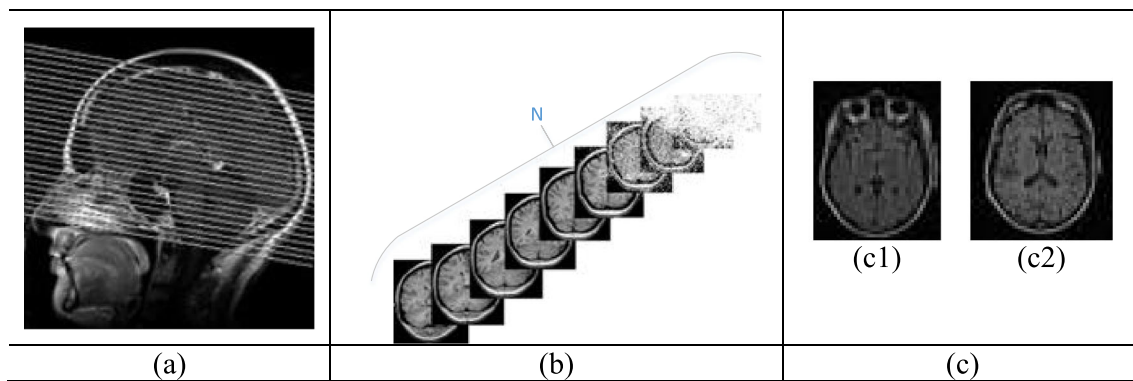
Fig. 7   **a** Brain scanning in MRI **b** Different slices in an MRI **c** Slice No. 20 in two different MRI c1 and c2

image to another, smoothly and continuously. DARTEL is a suitable tool aims to get more accurate inter-subject registration of brain images [81]. SPM software has DARTEL registration capability.

Voxel-based morphometry (VBM) VBM is a neuroimaging analysis technique that allows investigation of focal differences in brain anatomy, using the statistical approach of SPM [82]. This method first maps all the scans to a brain template and then constructs a statistical test for every voxel to identify the regional differences between the two groups. Usually VBM is performed for examining differences across subjects, but it may also be used to examine neuroanatomical differences between hemispheres detecting brain asymmetry.

FSL FSL is a comprehensive library of analysis tools for FMRI, MRI and DTI brain imaging data. It runs on Apple and PCs (both Linux, and Windows via a Virtual Machine), and is very easy to install. Most of the tools can be run both from the command line and as GUIs (point-and-click graphical user interfaces). It is used for Brain Extraction, Registration, Motion Correction and EPI Distortion (BET, FLIRT, MCFLIRT, PRELUDE & FUGUE), Segmentation &

Structural Statistics (FAST, FIRST, SIENA, FSL-VBM), FMRI Preprocessing and Model-Based Analysis (FEAT), Resting-State Analysis, ICA (MELODIC, dual regression), Resting-State Analysis, Network Modelling (FSLNets), Diffusion MRI Analysis (FDT, TBSS), Diffusion Tractography (FDT), Arterial spin labelling (ASL).

FreeSurfer FreeSurfer software [23] is an open source software suite for full processing stream of structural MRI data. Steffener et al. [40] investigated the effects of education and physical activities on brain aging by computing the regional volumes of cortical and subcortical gray matter using the FreeSurfer for segmentation. The capabilities of FreeSurfer include:

– Skull stripping, B1 bias field correction, and gray-white matter segmentation
– Reconstruction of cortical surface models (gray-white boundary surface and pial surface)
– Labeling of regions on the cortical surface, as well as subcortical brain structures
– Nonlinear registration of the cortical surface of an individual with a stereotaxic atlas
– Statistical analysis of group morphometry differences

Table 4   The current open preprocessing tools

| Name	URL	Programming Language
SPM	http://www.fil.ion.ucl.ac.uk/spm/	MATLAB, C
VBM	http://dbm.neuro.uni-jena.de/vbm/	MATLAB
FreeSurfer	https://surfer.nmr.mgh.harvard.edu/	–
FSL	https://fsl.fmrib.ox.ac.uk/fsl/fslwiki/	C#
NiftyReg	https://sourceforge.net/projects/niftyreg/	Python
NiftySeg	https://sourceforge.net/projects/niftyseg/	Python
ITK	https://itk.org/ITK/resources/software.html	Java
Elastix	http://elastix.isi.uu.nl/download.php	C++
DTI-TK	http://dti-tk.sourceforge.net/pmwiki/pmwiki.php?n=Downloads.Downloads	C#
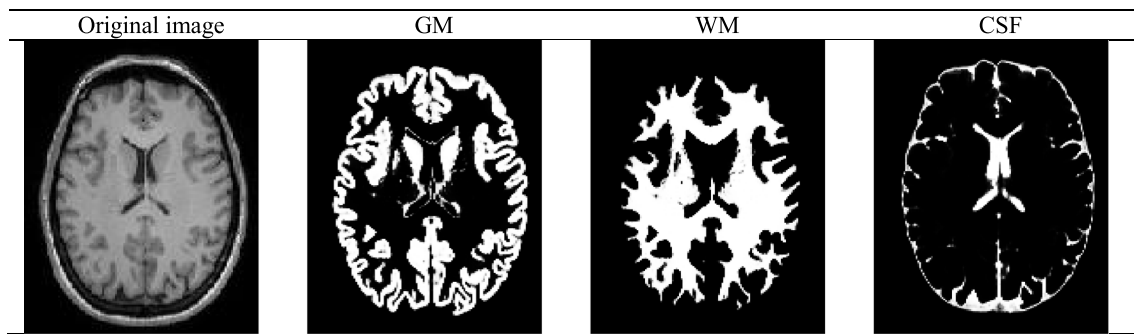
Fig. 8 Segmentation of a brain MRI into GM, WM, and CSF tissues by SPM

NiftyReg NiftyReg is open-source software for efficient medical image registration. It has been mainly developed by member of the Translational Imaging Group with the Centre for Medical Image Computing at University College London[4].

NifySeg NifySeg is the one of the project developed at University College London, which is licensed under BSD license. It a tool, which contains several programs to perform Expectation Maximization (EM) based segmentation of image n nifty or analyses format.

ITK or insight segmentation and registration Is an open-source, cross-platform system that provides developers with an extensive suite of software tools for image analysis [83]. In addition, ITK provide leading-edge segmentation and registration algorithm in two, three and more dimensions, it is distributed as an open-source software package [84].

Elastix Elastix is open source software, based on the well-known Insight Segmentation and Registration Toolkit (ITK). The software consists of a collection of algorithms that are commonly used to solve (medical) image registration problems. The modular design of Elastix allows the user to quickly configure, test, and compare different registration methods for a specific application [85].

DTI-TK DTI-TK is a spatial normalization and atlas construction toolkit optimized for examining white matter morphometry using DTI data. This software developed by Gary Zhang. In the year of 2011, a publication has been published in NeuroImage. It ranked DTI-TK as the top-performing tool in its class [86].

Dimensionality reduction

In most medical image datasets, a single sample is too huge and usually a large amount of dataset has redundancy. In these cases, some mathematical processes are employed to reduce the redundancy in a way that the most important information is saved. These processes are called dimensionality reduction [87]. The redundancy reduction techniques are placed in two main categories:

a) Feature selection: It is about selecting the most related and principle variables and keep them as the selected features in a new feature vector.

b) Dimension reduction: It is about extracting a new and smaller feature set [87].

Dimensionality reduction techniques are widely used in statistics and ML. As Table 5 shows, the mostly used dimensionality reduction method is Principle Component Analysis (PCA). PCA is a statistical process that reduces the data dimensionality by considering some linearly uncorrelated variables as Principle Components (PCs) [88].

MRI image segmentation

Segmentation of the more important parts of brain is a helpful way for brain diseases diagnosis, progression evaluation and checking the neurological circumstances. The traditional brain image segmentation is about manual segmentation of brain regions. This is a simple approach and is assumed to be the standard way of segmentation even today. However, it varies among personal opinions and requires considerable effort and time. Also, it is very time consuming and exceedingly requires human resource, thus impractical for large MRI data sets [89]. To deal with these problems, several automated segmentation tools were proposed such as SPM, FreeSurfer, etc. Many automated methods have been constructed for brain image segmentation. Generally, there are three classes of automated segmentation methods [90], 1) Traditional learning systems, 2) Neural Network and Deep Learning based systems and 3) Multi-atlas registration based methods. In the following, we describe each class briefly.

Traditional learning systems This class refers to ML based methods with handcrafted features. This kind of methods utilizes different classifiers to train a segmentation system and

---

Table 5 Summary of MRI based age prediction researches

Ref.	Preprocessing method	Brain image template	Location of research
[44]	SPM12, DARTEL	MNI152	Imperial College London, UK. King's College London, UK. Academic Medical Center, Amsterdam.
[61]	SPM8, DARTEL		Imperial College London, UK. Albert Einstein College of Medicine, US.
[62]	SPM12, DARTEL	MNI152	Imperial College London, UK.
[63]	Non-linear spatial regression		Imperial College London, UK. University of Edinburgh, UK. The University of Queensland, QLD, Australia.
[35]	1) N3 algorithm [80] 2) brain extraction with a multi-atlas method	–	Delft University of Technology, The Netherlands Erasmus MC, The Netherlands. Imperial College London, UK.
[36]	SPM2	ICBM152	Tohoku University, Japan.

[37]	1. Correction of image volumes
	2. Linear transformation into stereotaxic space
	3. Classification into GM, WM, CSF
	4. Smoothing the binary data into a range
	    of continuous data
	5. VBM analysis is performed
			Baycrest Centre for Geriatric
			    Care, Toronto, Canada.
			Maastricht University, The Netherlands.
			McGill University, Canada.
			University Hospital Maastricht,
			The Netherlands.

[41]	SPM2	ICBM152	National Tsing-Hua University, Taiwan Tohoku University, Japan South China University of Technology, China Tohoku Medical and Pharmaceutical University, Japan
[64]	SPM8, VBM8	standard space of Talairach and Tournoux	National University of Defense Technology, PR China.
[40]	FreeSurfer	–	Concordia University, Canada. Columbia University College of Physicians and Surgeons, USA. University of Florida, USA.
[39]	SPM8, VBM8	–	UCLA School of Medicine, USA Australian National University, Australia Jena University Hospital, Germany
[65]	SPM8, VBM8	–	University of Jena, Germany University Hospital Freiburg, Germany
[38]	–	–	The University of New South Wales, Australia

[45]	Structural MRI: FreeSurfer
	Functional MRI: Nipype
		–	Max Planck Institute for Human Cognitive
			    and Brain Sciences, Leipzig, Germany
			University of Leipzig, Germany
			Free University of Berlin, Germany
			Parietal project team - INRIA, Saclay, France
			CEA, DSV, I2BM, Neurospin, Gif-Sur-Yvette, France
			Kline Institute for Psychiatric Research, Orangeburg,
			    NY, USA
			Child Mind Institute, New York, NY, USA

[69]	SPM8	–	Beijing University of Technology, China
[32]	FreeSurfer	–	Ajou University, Suwon, South Korea Korea University, Seoul, South Korea Sungkyunkwan University, Seoul, South Korea Neuroscience Center, Samsung Medical Center, Seoul, South Korea

then use it for automatic segmentation such as what is done in [91]. Opbroek et al. proposed a brain tissue segmentation framework using Support Vector Machine (SVM) to train a system with manually labeled samples.

The main restriction of these methods is that handcrafted features usually suffer from limited representation capability for accurate recognition, considering the large variations of brain structures.

Neural network and deep learning based systems Neural networks and deep learning methods are broadly used in various studies to perform the tasks of segmentation, classification, detection and registration, on medical images [92]. The learning of these methods is based on the training data, such as CNNs in [17]. Zhang et al. proposed a CNN network for segmenting isointense stage brain tissues using multi-modality MR images.

Multi-atlas registration based methods A brain atlas is composed of serial sections along different anatomical planes of human brain where each relevant brain structure is assigned a number of coordinates to define its outline or volume. Atlases are developed to identify the major neuroanatomical structures of the entire brain on MRI scan, in both interactive digital technology and in print. It is intended that it would help in teaching, learning, testing, and in correlating lesions found on patients' MRI scans with anatomical structures [93]. For example, Multi-Atlas Label Fusion (MALF) is available for utilizing multiple reference atlases and was efficient in brain segmentation tasks [94].

Gray matter, is a major component of the central nervous system, and is distinguished from white matter based on cell bodies and myelinated axons. In neurology sciences, cortical thinning and intracortical gray matter volume losses are usual and are widely observed in normal ageing people, while it has a faster decreasing volume loss in subjects with neurodegenerative disorders such as Alzheimer's disease [38]. Moreover, the brain tissue atrophy formed by AD is more regionally particular than normal ageing [95].

A research [96] by studying fifty-four healthy volunteers (22 men, 32 women) aged 20–86 years underwent dual-echo fast spin-echo MR imaging investigated the relation between GM, WM and increasing age. Total GM, total WM, and intracranial space volumes were segmented by using MR image-based computerized semi-automated software. Volumes were normalized as a percentage of intracranial volume (%GM and %WM) to adjust for variations in head size. Age and sex effects were then assessed.

Both %GM and %WM in the intracranial space were significantly less in older subjects (≥50 years) than in younger subjects (<50 years). Consistently, %GM decreased linearly

with age, beginning in the youngest subjects. %WM decreased in a quadratic fashion, with a greater rate beginning only in adult midlife. Although larger GM volumes were observed in men before adjustments for cranium size, no significant differences in %GM or %WM were observed between the sexes.

This research concluded that GM volume loss appears to be a constant, linear function of age throughout adult life, whereas WM volume loss seems to be delayed until middle adult life. Both appear to be independent of sex [96].

A summary of researches in the area of MRI based age prediction is shown in Table 5, which all of them used structural T1-weighted images. In this table the preprocessing method or tool, the brain image template and the location of the research are shown (Table 6).

Prediction systems

A type of separating the whole implementation methods employed in various researches in the area of BAE is to divide them into researches used shallow classification algorithms or deep learning. In the following, some of the interesting investigations are described with more details.

Tables 7 and 8 display comparative analysis of the existing methods. Table 7 summarizes the most important of them. In this table, the type of learning method that can be classification or regression, the type of learning method, the method for feature selection sand dimension reduction, the used segment of the brain MRI, the employed evaluation metrics, and best achieved results of each research work are reported.

In another viewpoint, research works are categorized to three groups: pixel-based, voxel-based, and surface-based methods. Table 8 shows the best results achieved until now in each category. In addition, it is possible to make a comparison among various researches.

Figure 9 displays the categorization of the BAE systems into five categories based on the above-mentioned criteria.

Pixel-based, voxel-based, surface-based

The BAE systems can be categorized to pixel-based, voxel-based, and surface-based methods.

Table 6 The feature extraction tools

Name	URL	Programming Language
SURF	https://www.mathworks.com/help/vision/ref/detectsurffeatures.html	Matlab, Python, C#, C++
ORB	https://github.com/jl626/ORB-MATLAB	Matlab, Python
SIFT	https://robwhess.github.io/opensift/	Matlab, Python
BRIEF	https://github.com/abidrahmank/OpenCV2-Python-Tutorials/blob/master/source/py_tutorials/py_feature2d/py_brief/py_brief.rst	Matlab, Python

Table 7 Summary of researches using classification and regression methods for age prediction

Ref.	Type of learning method	Learning method	Feature selection & Dimension reduction	Brain volume	Evaluation metric	Best result
[44]	Classification Regression	DL (3D-CNN) GPR	–	GM WM Raw data	MAE r R² RMSE	In test, using GM in 3D-CNN: MAE=4.16 r=0.96, R²=0.92 RMSE=5.31
[61]	PRONTO + Regression	GPR	–	GM WM	MAE r R²	In train, using WM: MAE=6.16 r=0.922 R²=0.851 In validation, using GM: MAE=5.80 r=0.931 R²=0.867
[62]	Classification Regression	SVM SVR	–	GM	Accuracy MAE	Accuracy=96.25% MAE=5.08
[63]	Regression	GPR	–	Concatenated vectors of: GM WM	MAE r R² RMSE	In train: MAE=5.02 r=0.94 R²=88% RMSE=6.31 In test: MAE=7.08 r=−0.01 RMSE=8.85
[35]	Regression	Partial Least Squares (PLS) regression	–	–	–	Detailed in [35]
[36]	No learning	No learning	–	GM WM CSF Non-brain tissues	GM (mL) GMR (%)	–
[37]	No learning	No learning	–	GM WM CFS	–	–
[41]	Classification Regression	Based on VGG network Using small kernel size	–	–	MAE	MAE=4.0
[64]	Classification	SVM	A multivariate method based on sparse representation was used for voxel selection	GM WM CFS	Generalization Rate (GR) Sensitivity (SS) Specificity (SC)	GR=97.6% SS=100% SC=95.8%
[40]	No learning	No learning	–	GM (Cortical and subcortical)	–	Detailed in [39]
[39]	Regression	RVR	PCA	GM WM CFS	–	–
[65]	Regression	RVM	PCA	GM WM CFS	MAE RMSE r	In test, using GM: MAE=4.98 RMSE=6.28

Table 7 (continued)

Ref.	Type of learning method	Learning method	Feature selection & Dimension reduction	Brain volume	Evaluation metric	Best result
[38]	–	HMM	Vector Quantization (VQ)	GM WM CFS	Average Normalized age-Gap Error (ANGE) MAE RMSE	r = 0.92 ANGE = 2.57 MAE = 2.41
[45]	Regression	SVR RF regression	–	Non-determined	MAE	MAE = 4.29
[69]	–	Back Propagation Artificial Neural Network (BPANN)	PCA	GM WM CFS	MAE RMSE Mean Absolute Percentage (MAP)	MAE = 4.31 ±0.02 RMSE = 5.11 ±0.03 MAP = 7.34% ±0.01%
[32]	Regression	Ordinary Least Square (OLS) SGL GPR RVR DNN	SGL	–	MAE RMSE	Using combination of SGL & GPR: MAE = 4.05 RMSE = 5.16

One direction in creating BAE systems, is to use some of the image slices of brain MRI. In [41], a pixel-based approach is utilized and the number of used image slices are reported.

Both voxel-based and surface-based methods involve, in the first step, segmentation into GM, WM, and CSF. Voxel-based methods work directly on the voxel grid and are computationally very efficient, but they are less accurate since the resolution of voxel grid is limited. The other limitation of using it is less robustness to noise [33].

Surface-based methods usually construct a triangulated mesh based on either WM/GM boundary or GM/CSF boundary, which is then deformed to find the opposing boundary [33].

Classification and Regression

In the age estimation research area, classification means to categorize the data samples by the decade of the actual age. Classification can be done by shallow or deep classifiers.

Figure 10 illustrates the general process of a BAE system. In a BAE system, the input can be one or more slices and considering the number of slices, 2D or 3D CNN is used for modeling.

In the next subsection, the researches employed shallow and deep classification methods are reviewed.

Shallow learning algorithms for age estimation

The Gaussian Processes Regression (GPR) method has been shown to be applicable in age prediction. Cole et al. have studied the effects of Traumatic Brain Injury (TBI) [61] on brain structure by training a system with healthy individuals and check the system results for TBI patients. Statistical learning approach in PRoNTo is used for age prediction using the T1-weighted MRI images of 1537 healthy individuals gotten from eight publicly available sources. Next, a GPR is applied for the regression task to predict the actual chronological age.

Lancaster et al. utilize Bayesian optimization algorithm to find resampling and smoothing parameters due to have more suitable preprocessing factors [62]. The samples are divided into two groups of ages, <50 and >50 using SVM, and Support Vector Regression (SVR) was applied to predict the accurate chronological age.

In [97], the possibility of using neuroimaging data to get a biomarker of brain aging by ML methods is studied and it is concluded that neurodegenerative diseases cause the brain to get older, while activities like meditation and physical exercise cause to get smaller brain age. Cole et al. [63], use concatenated vectors of GM and WM segments to train a ML system based on GPR. By testing the trained system on samples with mentally diseases, Lothian Birth Cohort 1936 (LBC1936), the effects of mentally disorders have been shown.

Table 8 Summarization of the researches obtained best results for each certain data set

Dataset	Best achieved research	Learning method	Pixel-based/ Voxel-based	Best results
BANC	[44]	DL (3D-CNN) GPR	Voxel based	In test, using GM in 3D-CNN: MAE = 4.16 r = 0.96, R^2 = 0.92 RMSE = 5.31
8 public resources	[61]	GPR	Voxel based	In train, using WM: MAE = 6.16 r = 0.922 R^2 = 0.851 In validation, using GM: MAE = 5.80 r = 0.931 R^2 = 0.867
BAHC	[62]	SVM SVR	Voxel based	Accuracy = 96.25% MAE = 5.08
14 public resources	[63]	GPR	Voxel based	In train: MAE = 5.02 r = 0.94 R^2 = 88% RMSE = 6.31 In test: MAE = 7.08 r = − 0.01 RMSE = 8.85
Aoba	[41]	Based on VGG network Using small kernel size	Voxel based	MAE = 4.0
ICBM	[64]	SVM	Voxel based	GR = 97.6% SS = 100% SC = 95.8%
IXI	[65]	RVM	Voxel based	In test, using GM: MAE = 4.98 RMSE = 6.28 r = 0.92
ABSIS	[38]	HMM	–	ANGE = 2.57 MAE = 2.41
LIFE	[45]	SVR RF regression	Voxel based	MAE = 4.29

Cortical thickness estimation by MRI data is an effective way to diagnose and analyze the improvement of neurodegenerative diseases [33]. The recent investigation by [32], is about the prediction of brain age by cortical thickness data. The supervised model uses GPR method for regression task. But at first, the Sparse Group Lasso (SGL) method is utilized for feature selection. The SGL method is a well-known sparsity method used to prevent overfitting when only a subset of all features is enough to get the best prediction model. In addition, the final model is compared to a model based on Deep Neural Network (DNN).

Fig. 9 Categorization of the BAE systems into five categories, based on the learning methods (traditional or deep learning systems), based on used resources (pixel-based, voxel-based and surface-based methods)

Traditional learning Systems

Voxel- based methods   **Pixel-based methods**   **Surface-based methods**

Deep learning Systems
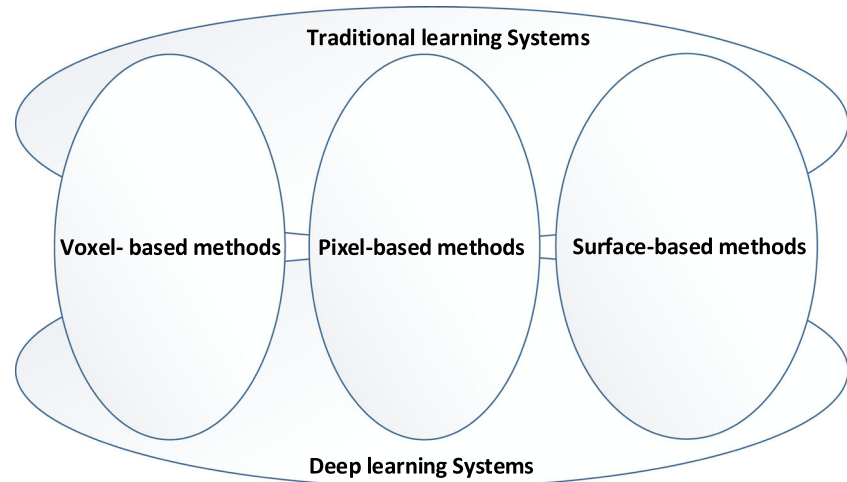
In [35], a preprocessing method, which corrects the non-uniformity of images, and an atlas-based method for brain extraction, is performed first. Then a mathematical modeling of age as a function is proposed to determine the brain morphology and distribution.

Some parameters, which can make the changes in GM, are studied in [36]. The MATLAB implementation of SPM2 is used for normalization and segmentation tasks to reach the volumes of GM, WM, CFS, and non-brain tissues. An entirely automated system is used to calculate the GMR, White Matter Ratio (WMR), and finally APC_{GMR}[5] with the proposed formula to analyze the important effects of gender, generational and cerebrovascular risk factors.

Tisserand et al. studied the age and some other parameters effects on the brain structure especially GM by Voxel-Based Morphometry (VBM) and the results detailed [37].

In [64], the relation between brain aging and grey matter volume is analyzed using structural MRI images. Since the spatial patterns of aging is dispersed in brain, various voxels of brain images are chosen to find the most distinguished parts of brain. After finding the appropriate voxels, the feature vectors are ready for classification using SVM.

In [39], a pattern recognition based approach known as (Relevance Vector Regression) RVR is trained on a large dataset with the GM images produced by SPM and the relation between brain age and meditation is analyzed.

In [65], a preprocessing and a dimension reduction method is applied on MRI images first. The regression method used for age estimation is Relevance Vector Machine (RVM). The proposed method could satisfactorily predict the actual age in healthy subjects and recognize AD patients well.

Hidden Markov Model (HMM) is also an approach of MRI based age prediction. In [38], the hidden states of model are created using wavelet coefficients and the transitions between

the states are estimated by vector quantization codebook. Other details are available in [38].

Liem et al. show that integrating multimodal MRI data, i.e., structural and functional images, would improve the age prediction accuracy [45]. The model is based on SVR and RF and the robustness and generalizability of it is tested using other large datasets and showed the head motion has not influence in final results.

Table 6 shows some tools for feature extraction from MRI images.

SURF or Speeded Up Robust Features is a patented algorithm used mostly in computer vision tasks and tied to object detection purposes.

Oriented FAST and rotated BRIEF (ORB) is a fast robust local feature detector, first presented by Rublee et al. in 2011, that can be used in computer vision tasks like object recognition or 3D reconstruction. It is based on the FAST keypoint detector and the visual descriptor BRIEF (Binary Robust Independent Elementary Features). Its aim is to provide a fast and efficient alternative to SIFT [98].

The scale-invariant feature transform (SIFT) is a feature detection algorithm in computer vision to detect and describe local features in images. Applications include object recognition, robotic mapping and navigation, image stitching, 3D modeling, gesture recognition, video tracking, individual identification of wildlife and match moving [99].

BRIEF is a general-purpose feature point descriptor that can be combined with arbitrary detectors. It is robust to typical classes of photometric and geometric image transformations [100].

Deep learning algorithms for age estimation

Some recent investigations have sought to use DL methods to utilize its advantages in order to have more accurate results and to decrease the preprocessing tasks. In addition, 3D-

---

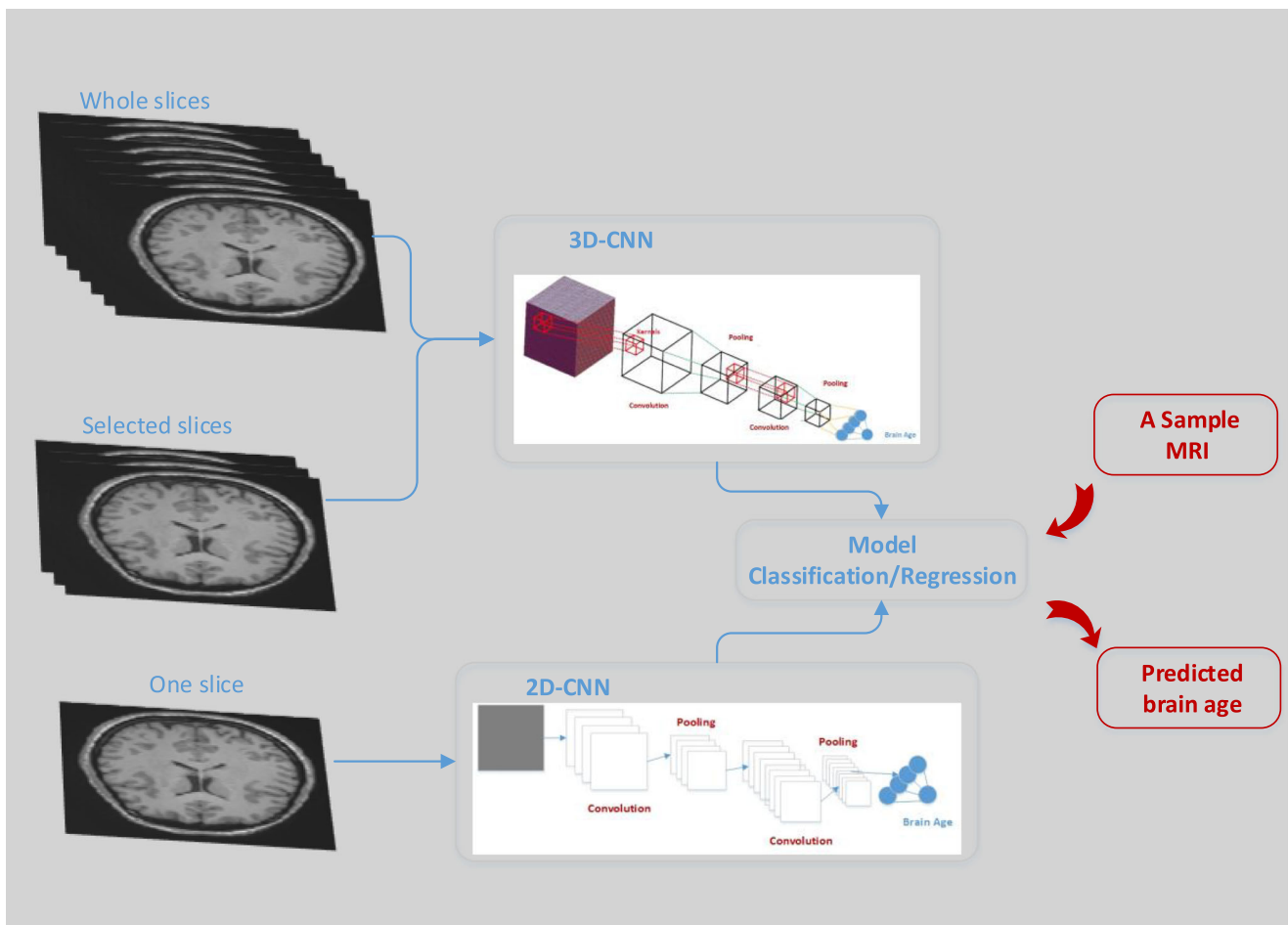[5] Annual percentage change in the GMR (APCGMR)

Fig. 10 General block diagram of employing CNN in a BAE system

CNNs are very appropriate deep methods for 3D types of data per sample, especially medical images such as NIfTI file formats of MRI, as like what has done in [44]. In [44], Cole et al. aim to use healthy samples to train a 3D-CNN for brain age prediction, find the heritability of it, and test the reliability of within-scanner and between-scanner samples. The samples to use are raw samples or preprocessed ones using SPM. Also, a GPR method is applied on all data samples to get some details of comparison between the results.

In [41], a DL based approach is proposed to predict individuals age by MRI images. CNN architecture is used and the detailed of implementation are explained. Classification is based on the (Visual Geometry Group) VGG network [101] and to gain the regression task, small kernel size is used in the network.

Lin et al. suggested a method to study the connectivity of the brain [69]. The PCA is performed for reducing data dimensionality and Back Propagation Neural Network (BPNN) is used for modeling a network of PCs. To improve the system performance, Genetic algorithm (GA) and Levenberg Marquardt (LM) algorithm are applied, too. The number of hidden layer neurons is set to seven.

The results of Table 8 show that in most of the researches voxel-based method result in higher performance.

Machine learning toolkits for medical image processing

DL methods are increasingly used to improve clinical practice. Among them, Convolutional neural networks can be used for efficiency improvement clinical practices since it is convenient in image-based tasks. There are some toolkits developed in medical imaging tasks. Table 9 shows some tools for classification and regression in BAE.

- *Scikit-learn*: provides a range of supervised and unsupervised learning algorithms via a consistent interface in Python. It is a free-to-use software covered by the BSD license. In scikit-learn, an estimator for classification is a Python object that implements the methods fit(X, y) and predict (T). An example of an estimator is the class sklearn.svm.SVC, which implements support vector classification.

Table 9 The classification and regression tools

Name	URL	Programming Language
scikit-learn	https://scikit-learn.org/stable/	Python, Cython, C and C++
PyTorch	https://pytorch.org/	Python
TensorFlow	https://www.tensorflow.org/	Python
Matlab	https://www.mathworks.com/	Matlab
R	https://www.r-project.org/	R
Rapid Miner	https://rapidminer.com/	Java
Knime	https://www.knime.com/knime-software/knime-analytics-platform	Java
Weka	https://www.cs.waikato.ac.nz/ml/weka/	Java
NiftyNet	https://github.com/NifTK/NiftyNet	Python
DLTK	https://github.com/DLTK/DLTK	Python

- *PyTorch*: is an open-source machine-learning library for Python, based on Torch, used for applications such as natural language processing.
- *TensorFlow*: is an end-to-end open source platform for machine learning. It has a comprehensive, flexible ecosystem of tools, libraries, and community resources that lets researchers push the state-of-the-art in ML and developers easily build and deploy ML powered applications.
- *MATLAB and Deep Learning Toolbox:* provide command-line functions and apps for creating, training, and simulating shallow neural networks. The apps make it easy to develop neural networks for tasks such as classification, regression (including time-series regression), and clustering.
- *R*: provides statistical linear and nonlinear modelling, regression, classification and clustering methods.
- *RapidMiner*: provides an environment for data preprocessing, machine learning, and deep learning. It supports all tasks of the machine learning modeling include data preparation, results visualization and model validation.
- *KNIME:* provides developed algorithms for machine learning and data mining includes preprocessing, for modeling, data analysis and visualization.
- *Weka:* It supports data preparation, classification, regression, clustering, association rules mining, and visualization tasks. In addition, it supports deep learning.
- *DLTK and NiftyNet:* In the area of MRI processing, DLTK, and NiftyNet, are two popular toolkits for analysis the brain images based on Deep Learning. DLTK and NiftyNet, are neural network toolkits written in python, on top of TensorFlow. DLTK is developed to enable fast prototyping with a low entry threshold and ensure reproducibility in image analysis applications, with a particular focus on medical imaging. Its goal is to provide the community with state of the art methods and models and to accelerate research in this exciting field. NiftyNet is an open-source CNN platform for research in medical image analysis and image-guided therapy. NiftyNet's modular structure is designed for sharing networks and pre-trained models.

Validation and Evaluation

The validation field is a part of a research by which the trained model performance is analyzed. Investigating the validation approaches, results in three general types of validation described below:

- *Bootstrapping*: A part of the completely training data may be selected randomly, for model validation, and the model is trained based on the remaining dataset. After getting the suitable performance, the model is trained with all dataset and got ready for testing with a new non-trained dataset.
- *k-fold cross validation*: The training dataset may be divided into k parts, and run the model by selecting one of the parts each time for test data. Finally, all of the results are gathered and a mean of them is reported as training performance. Then, the model is trained with all dataset and got ready for testing with a new non-trained dataset. This is called k-fold cross validation, where k is the number of dataset parts.
- The model is trained via all training set, and is validated with other dataset. This is a good approach to make generalizability and robustness [45].

Implemented methods for brain age prediction are placed in two general approaches, classification, and regression, as mentioned above and are evaluated by various formulas to calculate the model performance. In the area of age estimation problem, generally classification is the task to predict the age to the class of its decade (e.g. actual age = 76, truly predicted age class = 7), and regression is the task of age prediction to the actual chronological age. In other word, the result of a

classification model is a discrete value (e.g. decade of age or age stage like Teen or Adult) and the output of a regression model can be a real number with float point.

In [44], the researchers trained their models on 1600 MRI brain scans from healthy people between the age of 18 and 90 years old. They then used another 200 images to validate the process and tested the neural network on 200 other images it had never seen to determine how well it could measure the brain.

Table 5 shows the measures each research employed to evaluate its proposed method.

Classification model

In the following, the statistical measures for evaluating the performance of classification methods are described. True positive (TP), false positive (FP), True Negative (TN) and False Negative (FN) values are used for calculating most of the performance measures [102]. TP denotes the number of instances that belong to a class and recognized truly by the proposed modeling as the members of that class. FP denotes the number of instances that are wrongly recognized as the members of class, but they truly belong to other classes. TN is number of instances truly detected as do not belong to a class and FN is the number of instances that wrongly detected as not belonging to a class. Accuracy of a model (BAE system) is calculated by Eq. (1).

$$Accuracy : \frac{(TP + TN)}{(TP + TN + FP + FN)} \tag{1}$$

Sensitivity, also called the TP rate, recall, or probability of detection in some fields, measures the proportion of positives that are correctly identified and is computed by Eq. (2).

$$Recall : \frac{TP}{TP + FN} \tag{2}$$

Specificity also called the TN rate, precision, measures the proportion of negatives that are correctly identified and is computed by Eq. (3). F-measure is calculated based on precision and recall based on Eq. (4)

$$Precision : \frac{TP}{TP + FP} \tag{3}$$

$$F-measure : \frac{2*precision*recall}{precision + recall} \tag{4}$$

Figure 11 shows a sample confusion matrix when a classification method was used for MAE considering nine classes. In this table, for example, the gray cell shows that two samples which theirs chronological age is in the sixth decades were predicted as eighth decades. In this table, diagonal numbers, which are shown with bold face, are correct and the numbers of other cells show the error of BAE classification system.

Regression model

In the age prediction issue, there are some statistically based measures described in the sequel. These measures usually used when the modeling algorithm is a regression method. Correlation between chronological age and predicted age is calculated by Eq. (5) and total variance is obtained by Eq. (6).

$$r = Correlation \; (Pearson \; r) \tag{5}$$

$$R^2 = Total \; variance \tag{6}$$

Mean Absolute Error (MAE) is calculated by Eq. (7) and is used in several researches such as [41] that it method is able to predict subject's age with MAE of 4.0 years. Root Mean

Fig. 11 Relationship between chronological age and brain predicted age in a classification model

	Class	Actual (chronological age)
		1	**2**	**3**	**4**	**5**	**6**	**7**	**8**	**9**
Predicted age	**1**	**19**	3	0	0	1	0	1	0	1
	2	7	**112**	3	4	3	3	3	2	0
	3	0	3	**9**	1	2	0	1	0	1
	4	1	3	0	**24**	0	1	2	0	0
	5	0	1	2	0	**34**	1	4	0	0
	6	0	0	0	1	0	**28**	3	1	0
	7	1	2	0	0	2	4	**63**	11	2
	8	1	1	0	0	1	2	10	**43**	5
	9	0	0	0	0	0	1	2	0	**5**

Squared Error (RMSE) is another measure used for evaluating the performance of BAE systems and computed by Eq. (8).

$$MAE = \frac{\sum_{i=1}^{n}(y_i - x_i)}{n} \qquad (7)$$

$$RMSE = \sqrt{\frac{\sum_{i=1}^{n}(y_i - x_i)^2}{n}} \qquad (8)$$

Figure 12 shows a sample chart drawn when a regression method used for MAE. In this chat for example points A and B, are case that the brain age is lower and higher than the chronological age. If the sample cases are all healthy people's MRI, deviation from the identical line (dash line) shows the error of the BAE system.

Experiments

In existing BAE systems, three different usages of MRI images are considered as the following.

– Usage of all the slices
– Usage of some selected slices (reducing redundancies and less informational slices): In some research works like [41] some slices have been selected from a set of image slices in a MRI images, and the authors did not explain how and based on which measure they did so. For example, slices numbered 31, 39, 47, 55, 63, 71, 79, 87, 95, 103, 111, 119, 127, 135, and 143 that contain most of brain tissue are chosen as the input in [41].

– Usage of one significant slice: One image from middle tensor of MRI can be used for age prediction. However the result may not be enough accurate (e.g. [103]).

In our experiments, we investigate using of only one slice for experiment. In this regard, two approaches are used for feature extraction [104]. The age estimation task is performed on MRI images by extracting discriminating features and then SVM classification method is used to classify the ages into nine classes based on MRI images. Figure 13 illustrates the general view of this method.

Two approaches for feature extraction are described in the following. *C-SVDDNet* is a single layer network [105], which is an unsupervised feature-learning network towards robust and compact feature presentation. The main idea of Centered- Support Vector Data Description (SVDD) [106] is to learn good features from unlabeled data. It moves the centroid of SVDD ball [107] to the center of k-means, while paying attention to distribution and density of information. SVDD is an approach for clustering which attends not only to the center of data, but also to its distribution. It considers a sphere-shaped boundary named SVDD ball around data with specific center and radius, and for a new data with the same distances from two centers, the nearest ball surface would be preferred. To this end, the image is divided into some patches, each has a center and a radius, and after performing SVDD, the ball around data would move and centered to the k-means center, called C-SVDD center. The next step is to use a modified Scale Invariant Feature Transform (SIFT) descriptor,
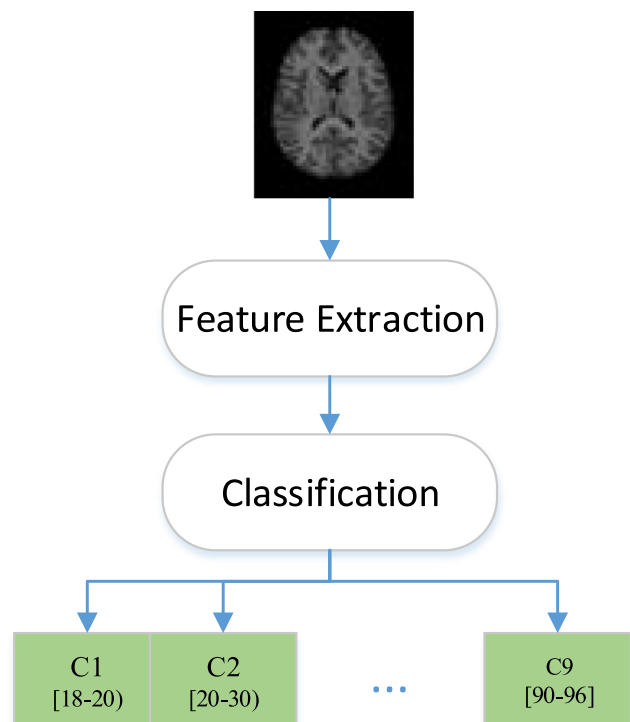

Fig. 12 Relationship between chronological age and brain predicted age in a regression model

Fig. 13 Block diagram of the method in [104]

which divides each feature map into $m \times m$ blocks and then only extracts an 8-bit gradient histogram from each block in the same way as SIFT does due to reduce dimensionality while preserving significant information. Figure 14 illustrates the general view of this method.

Complex Network is an approach to address edge detection issue based on local dimension of complex networks. The model is based on the Euclidian distance and the gray-level similarity indices to convert an image into complex networks. Since it is experiential that edge pixels have lower node dimension than non-edge pixels, it is used for edge detection [108]. We use this method for edge detection and extracting features from brain MRI images. Table 10 shows some samples employing this method of feature extraction.

In addition, some feature sets are provided to evaluate the proposed methods. Feature set 1 is obtained as follows. The second mentioned approach (based on the Complex Networks) is used to get edge-detected images. Then each edge-detected image of the dataset is placed into a 1-dimensional vector, by the way that rows of an image are inserted continuously in one unique row. Feature set 2 consists of mean and variance for each row of an image, instead of pixel values. Feature set 3 consists of feature set 1, but it additionally has the mean and variance for each eight neighbor rows of an image. Feature set 4 consists of Feature set 3, while it additionally has the values of mean and variance for each 16 neighbor rows of an image.

The classification method used here is SVM [109], a powerful method against small datasets and curse of dimension.

Experiments are on the Open Access Series of Imaging Study (OASIS), which contains MRI images of brain. The dataset consists of 416 right-handed subjects aged 18 to 96 and some of them are diagnosed to have Alzheimer Disease (AD). For 20 of the non-demented subjects, images are also included after a short delay (less than 90 days) for assessing reliability [106]. All images have 176×208 pixels. Table 11 shows number of image samples in each class.

Experimental results are shown in Table 12. 10-fold cross validation is used to compute accuracy. Table 12 shows the results of SVM on four feature sets extracted from Complex Network. It is observable that losing information of images, such as what is done during the process of edge detection, would lead to inaccurate results for this type of dataset. However, adding some information like mean and variance together for some blocks of images, like one row or some neighbor rows of them, would have more valuable information and the results will be improved.

In Table 12, bold face numbers show two highest achieved accuracies. As the results show raw data resulted in higher accuracy but on the other hand the dimension of the raw data is very high compared to the Feature set 3.

In another experiment, the raw data is given to SVM for classification despite of being unusual to do so, and got remarkable results as shown in Table 12. Furthermore, Table 13 provides the confusion matrix, and Fig. 15 is the error rate diagram of this approach. According to error rate diagram and confusion matrix, class 9 has the most error rate between others. It is more confused with class 8 that is not as vital as when it confused with class 1 or 3. The other remarkable issue, which is realized from confusion matrix, is about class 7 that is confused with all other classes at least once.

Discussion

Overview

BAE based on MRI images with high accuracy would have a great effect on early detection of neurodegenerative diseases, and would attract great attention from both academia and biology. Some of the bolded studies utilized ML techniques were discussed and summarized in this work. Most important works in this area are gathered and some tables are provided to compare them. The comparison of the mentioned works in the fields of dataset, preprocessing methods, learning methods, and the best achieved results are useful to get the remarks of a perfect BAE system. BAE could enable early detection of abnormal brain development in individuals with a family history of Alzheimer, diabetes, TBI, Parkinson, schizophrenia,
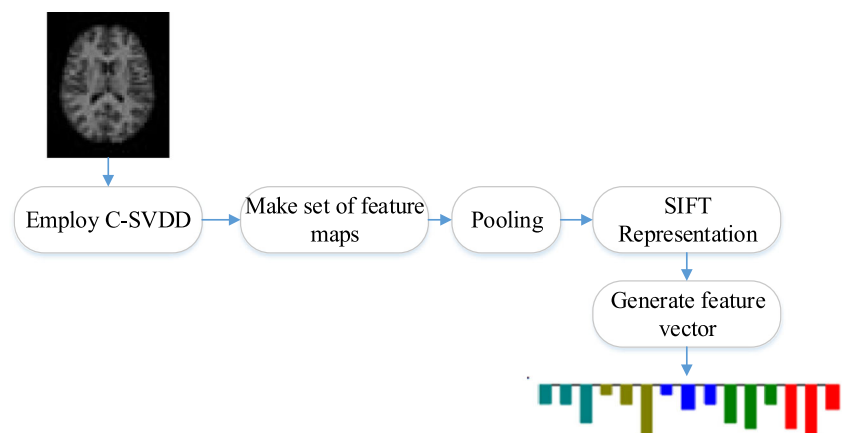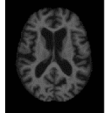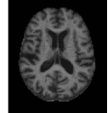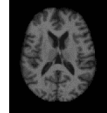
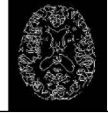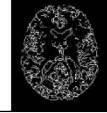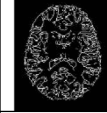**Fig. 14** The architecture of C-SVDDNet
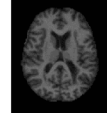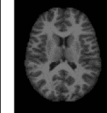
Table 10 Samples of MRI images in (first row) and the result of employing complex network on each image (second row)

MRI image					
result of employing complex network					
Age	90	78	68	57	21
Class	9	7	6	5	2

autism, or other heritable neurological disorder, those who have experienced early-onset neurological damage, and those who have been exposed prenatally to environmental toxins or substances of abuse. Of course, it is important to proceed cautiously, as much more research is needed to test the validity and cost-effectiveness of such approach [43].

On average, the model's prediction for a healthy individual should be in a small range within his or her chronological age. In a research, the average prediction error was 8 months for 3-year-olds (with the prediction ranging from 2 to 4 years) and 1.5 years for 20-year-olds (with the prediction ranging from approximately 17-23 years). The reason is, early in childhood, the anatomical differences between individuals are the strongest indicator of an individual's age.

Gray matter signal intensity within subcortical regions was the very strongest predictor during early and middle childhood, whereas diffusivity within subcortical regions of interest was the strongest predictor late in adolescence. By contrast, diffusivity within white matter fiber tracts was a consistently strong predictor across the age range. It is worth noting that total cortical area was a very poor predictor of age, exhibiting high variability across the age range [43].

Researchers from King's College London developed a deep learning system to measure brain age using raw data from an MRI scanner that can help reveal the onset of conditions such as dementia [44]. Cole et al. presented a 3D-CNN network to predict brain age and reported accurate results. They showed for the first time that 3D-CNN network can accurately estimate the brain age from MRI data.

Key aspects of achieving a good training system

In the following, some questions described in Introduction Section are answered and some directions are presented for the future works:

Q1: Is there any way to calculate brain age by brain MRI images?

Answer: There are several studies for BAE by MRI images. The increasing number of researches in this area shows the possibility of doing it. The investigations seek to reach more accurate and reliable results for BAE and neurological disease detection.

Q2: Do neurodegenerative diseases cause changes in brain structure?

Answer: There are several studies on the effects of neurodegenerative diseases on the brain ([40, 41, 44, 63]. The brain structure would get older by diseases like Alzheimer which is observed to have independent gray matter atrophy patterns with normal aging. Different regions of brain are affected by brain atrophy with aging [110].

Q3: Is it possible to specify the chronological age by brain age?

Answer: As mentioned before, some neurodegenerative diseases cause the brain morphology get older. By training an accurate BAE system, it is possible to predict the brain age. In the case, the brain age was greater than chronological age, there may be a disease, which affects

Table 11 The characteristics of the MRI images

class	Range	No. of samples	class	Range	No. of samples
1	[18-20)	29	6	[60-70)	40
2	[20-30)	125	7	[70-80)	89
3	[30-40)	14	8	[80-90)	57
4	[40-50)	30	9	[90–96]	14
5	[50-60)	43			

Table 12 Accuracy on 10 folds using raw data and feature set extracted by C-SVDDNet and Complex Network

Input of Classification	Accuracy (%)
raw data	*75.34*
Features extracted from C-SVDDNet	22.78
Feature set 1	26.27
Feature set 2	69.73
Feature set 3	*69.99*
Feature set 4	68.36

Table 13 Confusion Matrix using SVM on raw data

	Class	Actual								
		1	2	3	4	5	6	7	8	9
Predicted	1	**19**	3	0	0	1	0	1	0	1
	2	7	**112**	3	4	3	3	3	2	0
	3	0	3	**9**	1	2	0	1	0	1
	4	1	3	0	**24**	0	1	2	0	0
	5	0	1	2	0	**34**	1	4	0	0
	6	0	0	0	1	0	**28**	3	1	0
	7	1	2	0	0	2	4	**63**	11	2
	8	1	1	0	0	1	2	10	**43**	5
	9	0	0	0	0	0	1	2	0	**5**

the brain structure and makes it older. For healthy people in all the research works, it is assumed that chronological age and brain age is the same and the chronological age is considered as a label for a MRI brain sample, which contribute in building a BAE system.

Q4: What is a suitable approach for MRI based age prediction?

Answer: By looking at the groups of BAE approaches, there are two major approaches; those use shallow classification methods and those use DL methods. A convenient system is one, which have the ability to accurately estimate brain age, have generalization and robustness properties, and be executable over time and system hardware. To reach these goals, so many examinations around different databases, different system controlling parameters, and various system architectures are needed. In both groups of approaches, there are models, which achieved high accuracy results. Consequently, we cannot say strongly which one is the best for building a BAE system.

Q5: What are the requirements of such a system to predict brain age?

Answer: Several items exist to create an accurate BAE system. Using the statistical analysis of the images and having large training dataset would help greatly.
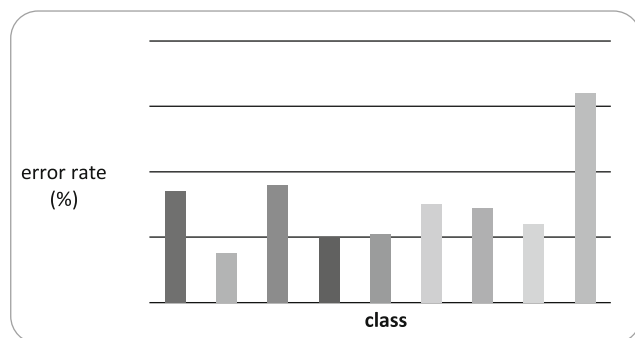

Fig. 15 Error rate (%) diagram for SVM based classification with no feature extraction

Q6: Which systems are more accurate? Pixel-based, voxel-based or surface-based?

Answer: In [33], an investigation is presented to compare the voxel-based and surface-based methods for cortical thickness estimation. Another existing approach is based on some of the MRI slices in axial direction, known as pixel-based methods. Pixel-based methods may employ various kinds of algorithms including shallow classification algorithms and deep learning to train an accurate model with the pixel-based data. By comparison of the most selected study results in the area of BAE, one may discuss about the much better approach. This is not a convenient comparison since the system accuracy is generally depends on the whole system architecture. A good ML system is the most compatible system with the training dataset and test dataset. Many other parameters exist to control system performance. For example, some of the parameters like the number of deep layers, number of nodes per layer, weights between nodes, activation function, learning rate, momentum, etc. are the major controlling parameters of deep systems.

Q7: Is spatial normalization, resampling, and spatial smoothing a necessary step in preprocessing?

Answer: A big problem in MRI researches is variation between instruments. We should have a way to measure the underlying tissue and not the instrumental bias to put samples all in a database.

Preprocessing methods of MRI images include bias-field correction, removal of non-brain tissue, tissue classification, motion correction, artifact removal, linear registration, non-linear registration, target image (e.g., atlas, average template), interpolation method, and smoothing kernel. As mentioned before, MRI scans should be preprocessed due to solve the problems of head motioning during scan and brain morphometric variations among people. The mentioned steps are usually done to deal with this problem. Although some techniques like DL methods do not necessarily need image preprocessing and are compatible with raw data, there are preprocessing soft wares prepared for medical images such as SPM. Furthermore, in most studies, using preprocessed images, and extracting suitable features from the training images yield more accurate results than raw data.

The impact of normalization and reslicing on the accuracy of BAE did not reported explicitly in the existing papers. However as it is obvious, removing useless parts of an MRI image can reduce complexity of modeling and instrumental bias and accordingly increase the accuracy of BAE.

Q8: Among GM, WM, and CSF, which is more significant in age prediction?

Answer: By looking at the extracted and used features in most investigations, it is obvious that GM has the most significant effect in BAE. Some researches in the area of brain age assessment in neurological and psychiatric diseases are summarized in [97], and it is obvious that more than 70% of them used GM for feature extraction.

Q9: In voxel-based systems, is the voxel size effective in age prediction?

Answer: Since the voxel is considered as the smallest informative volume of MRI, if the voxel size is large, the time complexity is lower but we may lose details and information. In contrast, if the volume size is small, we lose less information but the time complexity and redundant information is higher. Despite, the accuracy of a BAE system, is the main goal and the voxel size should be tuned so that the accuracy is the maximum. An investigation was provided to classify the young and old individuals, estimate the actual age, and optimize the resampling parameters [62]. In this investigation, some parameters such as smoothing kernel size and voxel size were optimized by Bayesian optimization algorithm. It is shown that optimizing the parameters would improve the total result.

Q10: Instead of using GM and WM, can we use smaller parts of the brain?

Answer: Aging process has some effects on brain, which differ between individuals. The manner of brain aging is not completely clear yet. Brain changes do not occur to the same extent in all brain regions. Also, there are changes in GM and WM during aging process and in different lobes, too. Accordingly, the aging affects the whole brain structure. Furthermore, to extend the created models for neurological diseases detection, the whole brain structure would help well.

So far, some researches have been used only one slice of MRI, some selected slices or whole the slices of MRI images in raw for BAE. Some other researches have segmented MRI images into WM, GM and CSF and used GM and WM for BAE. However other information like description of corpus callosum, volume of brain and other descriptors can be employed in future research works.

The results of a recent research show that the longitudinal dimensions of Corpus Callosum (CC) are larger in the elderly, while the younger subjects have significantly thicker callosal dimensions [111]. This hint can be considered for BAE. CC area has the potential of being a Region of Interest (ROI) in preprocessing and modeling in future works.

A longitudinal study over regional brain volumes indicates that the effects of age are not uniform across brain regions [112]. Therefore considering regional MRI processing and selection of some ROI may enhance the results of a BAE system.

Q11: Are atlas-based methods useful in BAE?

Answer: Multi atlas based methods have been used for detection of Alzheimer disease in recent years ([113–115]. Multi atlas based morphometry is used for measuring morphometric representations of the same image in different spaces of multiple atlases. However, in the task of BAE, most of the researches have used the whole brain tissues, or the segmentation of it into GM and WM by specific software like SPM, FSL, etc. Therefore, the effectiveness of atlas-based method in BAE has not been studied until now.

Q12: What is the best result achieved for BAE?

Answer: Some MAE values reported in different investigations are about 4 years as observed in the previous sections. The MAE value in [38] is 2.16 which is based on the hidden Markov model. It is possible for the researchers to study the existing methods and compare the results. However, it should be noted that the investigations are not all on the same datasets with the same sizes in training and test. In this situation, it is not fair to report the one with the lowest MAE as the best system.

Q13: What is the convenient size of training data?

Answer: Generally, DL systems require large dataset due to have enough data to set the system weights properly. On the other hand, some approaches like SVM are more compatible with small amount of dataset [104]. It is a major task to create a robust and extensible system to reach the generalization property.

Q14: What are the challenges and solutions in brain age prediction?

Answer: This question will discuss in the next section with details.

Q15: What can brain MRI imaging produced as quantitative and qualitative descriptions for predicting age?

Answer: Actually, none of the researches in BAE field has been focused on quantitative and qualitative descriptions extracted from brain MRI images for predicting age. Volume of GM, WM, and CSF are the quantitative measures those are resulted from MRI segmentation.

The development has the potential to significantly influence the way clinicians come to a diagnosis. There is considerable evidence that conditions such as diabetes, schizophrenia, and traumatic brain injury are correlated with faster brain aging. So a way to measure brain aging quickly and accurately could have an important impact on the way clinicians deal with these conditions in the future. Brain-predicted age represents an accurate, highly reliable, and genetically valid phenotype that has potential to be used as a biomarker of brain

aging, mentions Giovanni Montana of King's College London in their research paper.

Challenges

The age prediction algorithms should be fast and accurate. In the following, we describe the challenges the researchers face with in BAE.

Data sets Larger number of samples, size of each sample (e.g. about 150 high-resolution images) and data variation (e.g. the angle of patient head from the MRI device, different size of heads, etc.) in training dataset are the most major factors in training a ML system precisely. Collecting MRI examples in medical centers or clinics is not a straightforward work. Collecting large number of examples make this work more challenging. Another point is usually the persons refer to clinic to capture MRI images have a brain disease and healthy people seldom refer for MRI imaging, while a model for BAE is built based on health brain images. Therefore, collecting MRI images from healthy persons makes the work harder.

Prediction time Table 14 shows the age estimation time reported in the papers. As can be seen this time can be reduced by running the program on GPU system. Generally, DL methods need a huge time of training.

In [41] a deep learning method was used to predict subject's age. Compared with previous methods, the algorithm achieved comparable accuracy using fewer input images. With GPU-based version of the program, the time required to make a prediction is 20 ms.

Using CUDA, TITAN X GPUs and cuDNN with the Torch deep learning framework in [44], the trained deep learning method is able to give the brain age in seconds with a MAE of nearly 4.5 years. This analysis would typically take a neuroscientist more than 24 h [44].

Hardware Computing on large amount of data specially using DL methods requires suitable hardware with high power of computation and large volume of memory. Broadly, the computation runs on GPU systems in parallel, decreases the time of BAE modeling and prediction significantly.

Accuracy To have an applicable BAE system the most important challenge is similarity between images of persons with different ages [116], and thus a strong technique would necessarily be used to obtain good results, though learning good features. The challenge is that the images look very similar and classification/regression would have difficulties because of very small interclass changes.

Solutions

Some solutions and directions to cope with the mentioned challenges in the previous subsection are as the follows:

Data sets in some researches some available datasets are combined together to build a larger dataset. Although, this work could produce a larger dataset, this is a challenging work because the parameters of imaging for each dataset could have different values compared to other datasets. Modeling based on a dataset with larger number of examples can have higher degree of generalization and more trustable.

Hardware Computation on a huge training dataset requires running system program on high performance servers. In addition, several cloud systems are available to store the huge amount of data and process huge datasets. An alternative to run program on a high performance hardware is reducing the computation. However, this reduction was not the subject of published research works so far. Using only the most informative slices of MRI instead of using all the slices is one way of computation reduction. Under sampling in three dimensions, while maintaining the vital information, is another way of time complexity reduction.

Accuracy Most of the deep learning methods require large number of examples and to achieve high accuracy or low amount of MAE, merging the datasets is an applicable solution.

Table 14 Age estimation time, train time for building model and test time for one test sample

Ref.	Method	Train time		Test time	Comment	Implementation language
[44]	DL (3D-CNN)	GM/WM	18 h	290-940 ms	Using four GPUs	Torch
		GM + WM	42 h			
		Raw data	83 h			
[41]	Based on VGG network	12 h		200 ms	CPU	
				20 ms	GPU	

Based on the results of researches, voxel-based features that reserve more features than pixel-based features could perform better than the other methods.

Using transfer learning [117] from pre-trained models is another choice that has not been applied for BAE problem so far but the results in several applications illustrate that it has capability to boost the accuracy and reduce the computational cost.

Conclusion and future work

During the past decades, there has been a substantial growth of interest in BAE. It was the main purpose of this paper to draw attention to those approaches that contribute to estimation of age based on MRI images in different ways. At first, the characteristics and roles of extracted features from different datasets were discussed. Moreover, based on the machine learning methods, we categorized them into two groups, including deep learning based approaches, and traditional machine learning based approach. Although many measures and techniques have been proposed to age estimation, each of them has its own strengths and weaknesses, which were discussed in details at the end of each section. Furthermore, we systematically summarized and compared the contributions of studies with a critical perspective and defined the possible challenges and future research directions.

With the proliferation of various available data and rich features in describing the changeable part of brains in neurodegenerative disease, finding a high-performance age estimation system has been becoming challenging for existing studies. The complexity of system is originated from the availability of high dimensional data resources.

To reduce the redundancy and hence computational complexity, in our future experiments, we are going to select some slices automatically based on a measure.

Compliance with ethical standards

Conflict of interest On behalf of all authors, the corresponding author states that there is no conflict of interest.

References

1. Jana, R., Datta, D., and Saha, R., Age Estimation from Face Image using Wrinkle Features. Procedia Computer Science 46:1754–1761, 2015.

2. Ng, C., Yap, M., Cheng, Y., and Hsu, G., Hybrid Ageing Patterns for face age estimation. Image Vis. Comput. 69:92–102, 2018.

3. Antipov, G., Baccouche, M., Berrani, S., and Dugelay, J., Effective training of convolutional neural networks for face-based gender and age prediction. Pattern Recogn. 72:15–26, 2017.

4. Liu, H., Lu, J., Feng, J., and Zhou, J., Group-aware deep feature learning for facial age estimation. Pattern Recogn. 66:82–94, 2017.

5. Xing, J., Li, K., Hu, W., Yuan, C., and Ling, H., Diagnosing deep learning models for high accuracy age estimation from a single image. Pattern Recogn. 66:106–116, 2017.

6. Lee, J. W., Choung, C. M., Jung, J. Y., Lee, H. Y., and Lim, S. K., A validation study of DNA methylation-based age prediction using semen in forensic casework samples. Legal Med. 31:74–77, 2018.

7. Lee, H. Y., Jung, S. E., Oh, Y. N., Choi, A., Yang, W. I., and Shin, K. J., Epigenetic age signatures in the forensically relevant body fluid of semen: a preliminary study. Forensic Science International: Genetics 19:28–34, 2015.

8. Jang, H., Shin, W., Lee, J., and Do, J., CpG and Non-CpG Methylation in Epigenetic Gene Regulation and Brain Function. Genes 8(6):148, 2017.

9. Naue, J., Hoefsloot, H. C. J., Mook, O. R. F., Rijlaarsdam-Hoekstra, L., van der Zwalm, M. C. H., Henneman, P., Kloosterman, A. D., and Verschure, P. J., Chronological age prediction based on DNA methylation: Massive parallel sequencing and random forest regression. Forensic Science International: Genetics 31:19–28, 2017.

10. Maggio, A., The skeletal age estimation potential of the knee: Current scholarship and future directions for research. Journal of Forensic Radiology and Imaging 9:13–15, 2017.

11. Monum, T., Mekjaidee, K., Pattamapaspong, N., and Prasitwattanaseree, S., Age estimation by chest plate radiographs in a Thai male population. Sci. Justice 57:169–173, 2017.

12. Darmawan, M. F., Yusuf, S. M., Kadir, M. R. A., and Haron, H., Age estimation based on bone length using 12 regression models of left hand X-ray images for Asian children below 19 years old. Int. J. Legal Med. 17:71–78, 2015.

13. Schmidt, S., Nitz, I., Ribbecke, S., Schulz, R., Pfeiffer, H., and Schmeling, A., Skeletal age determination of the hand: a comparison of methods. Int. J. Legal Med. 127:691–698, 2013.

14. Schmeling, A., Schulz, R., Reisinger, W., Muhler, M., Wernecke, K. D., and Geserick, G., Studies on the time frame for ossification of the medial clavicular epiphyseal cartilage in conventional radiography. Int. J. Legal Med. 118:5–8, 2004.

15. Wittschieber, D., Schulz, R., Vieth, V., Kuppers, M., Bajanowski, T., Ramsthaler, F. et al., The value of sub-stages and thin slices for the assessment of the medial clavicular epiphysis: a prospective multi-center CT study. Forensic Science, Medicine, and Pathology. 10:163–169, 2014.

16. Wittschieber, D., Ottow, C., Vieth, V., Kuppers, M., Schulz, R., Hassu, J. et al., Projection radiography of the clavicle: still recommendable for forensic age diagnostics in living individuals? Int. J. Legal Med. 129:187–193, 2015.

17. Zhang, K., Chen, X. G., Zhao, H., Dong, X. A., and Deng, Z. H., Forensic age estimation using thin-slice multidetector CT of the clavicular epiphyses among adolescent Western Chinese. J. Forensic Sci. 60:675–678, 2015.

18. Cameriere, R., Giuliodori, A., Zampi, M., Galic, I., Cingolani, M., Pagliara, F. et al., Age estimation in children and young adolescents for forensic purposes using fourth cervical vertebra (C4). Int. J. Legal Med. 129:347–355, 2015.

19. Nagaoka, T., and Kawakubo, Y., Using the petrous part of the temporal bone to estimate fetal age at death. Forensic Sci. Int. 248:188 e1–188 e7, 2015.

20. de Oliveira, F. T., Soares, M. Q., Sarmento, V. A., Rubira, C. M., Lauris, J. R., Rubira-Bullen, I. R. et al., Int. J. Legal Med. 129: 195–201, 2015.

21. Ge, Z. P., Ma, R. H., Li, G., Zhang, J. Z., and Ma, X. C., Age estimation based on pulp chamber volume of first molars from cone-beam computed tomography images. Forensic Sci. Int. 253:133.e1–133.e7, 2015.

22. Lewis, A. J., Boaz, K., Nagesh, K. R., Srikant, N., Gupta, N., Nandita, K. P. et al., Demirjian's method in the estimation of age: a study on human third molars. J. Forensic Dent. Sci. 7: 153–157, 2015.

23. Surfer, 2018. https://surfer.nmr.mgh.harvard.edu/, Accessed date: 6/8/2018.

24. Talabani, R. M., Baban, M. T., and Mahmood, M. A., Age estimation using lower permanent first molars on a panoramic radiograph: a digital image analysis. J. Forensic Dent. Sci. 7:158–162, 2015.

25. Scoles, P. V., Salvagno, R., Villalba, K., and Riew, D., Relationship of iliac crest maturation to skeletal and chronologic age. J. Pediatr. Orthop. 8:639–644, 1998.

26. Wittschieber, D., Vieth, V., Domnick, C., Pfeiffer, H., and Schmeling, A., The iliac crest in forensic age diagnostics: evaluation of the apophyseal ossification in conventional radiography. Int. J. Legal Med. 127:473–479, 2013a.

27. Wittschieber, D., Vieth, V., Wierer, T., Pfeiffer, H., and Schmeling, A., Cameriere's approach modified for pelvic radiographs: a novel method to assess apophyseal iliac crest ossification for the purpose of forensic age diagnostics. Int. J. Legal Med. 127:825–829, 2013b.

28. Buckberry, J. L., and Chamberlain, A. T., Age estimation from the auricular surface of the ilium: a revised method. Am. J. Phys. Anthropol. 119:231–239, 2002.

29. Eich, G. F., Babyn, P., and Giedion, A., Pediatric pelvis: radiographic appearance in various congenital disorders. RadioGraphics 12:467–484, 1992.

30. Hao, D., Xiren, X., and Rubiao, P., The evaluation of the apophyseal ossification in conventional radiography in Hai Nan Han Group. Forensic Science and Technology 6:24–26, 1996.

31. Bunge, S. A., and Whitaker, K. J., Brain Imaging: Your Brain Scan Doesn't Lie About Your Age. Curr. Biol. 22(18):R800–R801, 2012.

32. Aycheh, H. M. et al., Biological Brain Age Prediction Using Cortical Thickness Data: A Large Scale Cohort Study. Front. Aging Neurosci. 10:252, 2018.

33. Clarkson, M. J. et al., A comparison of voxel and surface based cortical thickness estimation methods. Neuroimage 57(3):856–865, 2011.

34. Peters, R., Ageing and the brain. Postgrad. Med. J. 82(964):84–88, 2006.

35. Huizinga, W., Poot, D. H. J., Vernooij, M. W., and Roshchupkin, G. V., A spatio-temporal reference model of the aging brain. NeuroImage 169:11–22, 2018.

36. Taki, Y., Kinomura, S., Sato, K., and Goto, R., A longitudinal study of gray matter volume decline with age and modifying factors. Neurobiol. Aging 32:907–915, 2011.

37. Tisserand, D. J., van Boxtel, M. P. J., Pruessner, J. C., Hofman, P., Evans, A. C., and Jolles, J., A Voxel-based Morphometric Study to Determine Individual Differences in Gray Matter Density Associated with Age and Cognitive Change Over Time. Cereb. Cortex 14:966–973, 2004.

38. Wang, B., and Pham, T. D., MRI-based age prediction using hidden Markov models. J. Neurosci. Methods 199:140–145, 2011.

39. Luders, E., Cherbuin, N., and Gaser, C., Estimating brain age using high-resolution pattern recognition: Younger brains in long-term meditation practitioners. NeuroImage 134:508–513, 2016.

40. Steffener, J., Habeck, C., O'Shea, D., Razlighi, Q., Bherer, L., and Stern, Y., Differences between chronological and brain age are related to education and self-reported physical activity. Neurobiol. Aging 40:138–144, 2016.

41. Huang, T., Chen, H., Fujimoto, R., Ito, K., Wu, K., Sato, K., Taki, Y., Fukuda, H., and Aoki, T., Age estimation from brain MRI images using deep learning. Melbourne: IEEE 14th International Symposium on Biomedical Imaging, 2017

42. Dosenbach, N. U. F., Nardos, B., Cohen, A. L., Fair, D. A., Power, J. D., Church, J. A., Nelson, S. M., Wig, G. S., Vogel, A. C., Lessov-Schlaggar, C. N. et al., Prediction of individual brain maturity using fMRI. Science 329:1358–1361, 2010.

43. Brown, T. T., Kuperman, J. M., Chung, Y., Erhart, M., McCabe, C., Hagler, D. J., Venkatraman, V. K., Akshoomoff, N., Amaral, D. G., Bloss, C. S. et al., Neuroanatomical assessment of biological maturity. Curr. Biol. 22:1693–1698, 2012.

44. Cole, J. H., Poudel, R. P. K., Tsagkrasoulis, D., Caan, M. W. A., Steves, C., Spector, T. D., and Montana, G., Predicting brain age with deep learning from raw imaging data results in a reliable and heritable biomarker. NeuroImage 163:115–124, 2017.

45. Liem, F., Varoquaux, G., Kynast, J., Beyer, F. et al., Predicting brain-age from multimodal imaging data captures cognitive impairment. NeuroImage 148:179–188, 2017.

46. Meng, X., Jiang, R., Lin, D., Bustillo, J., Jones, T., Chen, J., Yu, Q., Du, Y., Zhang, Y., Jiang, T., Sui, J., and Calhoun, V. D., Predicting individualized clinical measures by a generalized prediction framework and multimodal fusion of MRI data. NeuroImage 145:218–229, 2017.

47. Bowman, F. D. B., Brain imaging analysis. Annual Review of Statistics and its Application 1:61–85, 2014.

48. Beheshti, I., and Demirel, H., Feature-ranking-based Alzheimer's disease classification from structural MRI. Magn. Reson. Imaging 34:252–263, 2016.

49. Kumar, S., Dabas, C., and Godara, S., Classification of Brain MRI Tumor Images: A Hybrid Approach. Procedia Computer Science 122:510–517, 2017.

50. Lu, W., Li, Z., and Chu, J., A novel computer-aided diagnosis system for breast MRI based on feature selection and ensemble learning. Comput. Biol. Med. 83:157–165, 2017.

51. Linna, K. A., Gaonkarc, B., Satterthwaiteb, T. D., Doshic, J., Davatzikosc, C., and Shinoharaa, R. T., Control-Group Feature Normalization for Multivariate Pattern Analysis of Structural MRI Data using the Support Vector Machine. NeuroImage 132: 157–166, 2016.

52. Mohsen, H., El-Dahshan, E. A., El-Horbaty, E. M., and Salem, A. M., Classification using Deep Learning Neural Networks for Brain Tumors. Future Computing and Informatics Journal 3(1): 68–71, 2018.

53. Pashaei, A., Sajedi, H., and Jazayeri, N., Brain tumor classification via convolutional neural network and extreme learning machines, 2018 8th International Conference on Computer and Knowledge Engineering, ICCKE, 8566571, pp. 314-319, 2018.

54. Berger, A., Magnetic resonance imaging. Br. Med. J. 324:35, 2002.

55. Case Western Reserve University, 2018. http://casemed.case.edu/clerkships/neurology/Web%20Neurorad/MRI%20Basics.htm. Accessed date: 9/11/2018.

56. Pooley, R. A., AAPM/RSNA Physics Tutorial for Residents. RadioGraphics 25(4):1087–1099, 2005.

57. Chau, W., and McIntosh, A. R., The Talairach coordinate of a point in the MNI space: how to interpret it. NeuroImage 25(2): 408–416, 2005.

58. Bakir, B., Sanli, S., Bakir, V. L., Avas, S. et al., Role of diffusion weighted MRI in the differential diagnosis of endometrial cancer, polyp, hyperplasia, and physiological thickening. Clin. Imaging 41:86–94, 2017.

59. Brennan, M. E., McKessar, M., Snook, K. et al., Impact of selective use of breast MRI on surgical decision-making in women with

newly diagnosed operable breast cancer. Breast 32:135–143, 2017.

60. Eiber, M., Weirich, G., Holzapfel, K., Souvatzoglou, M. et al., Simultaneous 68Ga-PSMA HBED-CC PET/MRI Improves the Localization of Primary Prostate Cancer. Eur. Urol. 70:829–836, 2016.

61. Cole, J., Cole, H., Leech, R., and Sharp, D. J., Prediction of Brain Age Suggests Accelerated Atrophy after Traumatic Brain Injury. Ann. Neurol. 77:571–581, 2015.

62. Lancaster, J., Lorenz, R., Leech, R., and Cole, J. H., Bayesian Optimization for Neuroimaging Pre-processing in Brain Age Prediction. Front. Aging Neurosci. 10:28, 2018. https://doi.org/10.3389/fnagi.2018.00028 eCollection 2018.

63. Cole, J. H., Ritchie, S. J., Bastin, M. E., and Hernández, M. C. V., Brain age predicts mortality. Mol. Psychiatry 23:1385–1392, 2018.

64. Su, L., Wang, L., Shen, H., and Hu, D., Age-related Classification and Prediction Based on MRI: A Sparse Representation Method. Procedia Environ. Sci. 8:645–652, 2011.

65. Franke, K., Ziegler, G., Klöppel, S., and Gaser, C., Estimating the age of healthy subjects from T1-weighted MRI scans using kernel methods: Exploring the influence of various parameters. NeuroImage 50:883–892, 2010.

66. Gaser, C., Volz, H. P., Kiebel, S., Riehemann, S., and Sauer, H., Detecting structural changes in whole brain based on nonlinear deformations-application to schizophrenia research. NeuroImage 10:107–113, 1999.

67. Loeffler, M., Engel, C., and Ahnert, P., The LIFE-Adult-Study: objectives and design of a population-based cohort study with 10,000 deeply phenotyped adults in Germany. BMC Public Health 15:691, 2015.

68. Nooner, K., Colcombe, S. J., Tobe, R. H. et al., The NKI-Rockland Sample: A Model for Accelerating the Pace of Discovery Science in Psychiatrym. Front. Neurosci. 6:152, 2012.

69. Lin, L., Jin, C., Fu, Z., Zhang, B., Bin, G., and Wu, S., Predicting healthy older adult's brain age based on structural connectivity networks using artificial neural networks. Comput. Methods Prog. Biomed. 125:8–17, 2016.

70. Larobina, M., and Murino, L., Medical image file formats. J. Digit. Imaging 27(2):200–206, 2014.

71. Sonka M., Hlavac, V., and Boyle, R., Image pre-processing. In: Image Processing, Analysis and Machine Vision. Boston: Springer, 1993.

72. Krig, S., Image Pre-Processing. In: Computer Vision Metrics. Berkeley: Apress, 2014.

73. Jude Hemanth, D., and Anitha, J., Image Pre-processing and Feature Extraction Techniques for Magnetic Resonance Brain Image Analysis. In: Kim, T., Ko, D., Vasilakos, T., Stoica, A., Abawajy, J. (eds) Computer Applications for Communication, Networking, and Digital Contents. FGCN 2012. Communications in Computer and Information Science, vol 350. Berlin: Springer, 2012.

74. Bo, Z., Jalal, M. F., and Jean-Luc, S., Wavelets, ridgelets and curvelets for Poisson noise removal. IEEE Trans. Image Process. 17(7):1093–1108, 2008.

75. Marianne, M., Russell, G., Jorg, S., Albert, M., and Mark, S., Learning a classification based glioma growth model using MRI data. J. Comput. 1(7):21–31, 2006.

76. Nicu, S., and Michael, S.L., Wavelet based texture classification. In: 15th International Conference on Pattern Recognition. 3: 3959–3962, 2000.

77. Manjón, J. V., MRI Preprocessing. In: Martí-Bonmatí L., Alberich-Bayarri A. (eds) Imaging Biomarkers. Cham: Springer, 2017.

78. Guo, C., Machine Learning Methods for Magnetic Resonance Imaging Analysis, 2012. PhD thesis, University of Michigan.

79. SPM webpage, https://www.fil.ion.ucl.ac.uk/spm/, Accessed date: 8/4/2018.

80. Tustison, N. J., Avants, B. B., Cook, P. A., Zheng, Y., Egan, A., Yushkevich, P. A., and Gee, J. C., N4ITK: improved N3 bias correction. IEEE Trans. Med. Imaging 29(6):1310–1320, 2010. https://doi.org/10.1109/TMI.2010.2046908.

81. Ashburner, J., A fast diffeomorphic image registration algorithm. NeuroImage 38(1):95–113, 2007.

82. Ashburner, J., and Friston, K., Voxel-based morphometry—the methods. NeuroImage 11:805–821, 2000.

83. Liu, Y., Kot, A., Drakopoulos, F., Yao, C., Fedorov, A., Enquobahrie, A., and Chrisochoides, N. P., An ITK implementation of a physics-based non-rigid registration method for brain deformation in image-guided neurosurgery. Frontiers in Neuroinformatics 8:33, 2014.

84. Johnson, H. J., McCormick, M. M., and Ibanez, L., The ITK software guide book 1: Introduction and development guidelines fourth edition updated for ITK version 4.7. Clifton Park: Kitware, Inc., 2015.

85. Mengler, L., Khmelinskii, A., Diedenhofen, M., Po, C., Staring, M., Lelieveldt, B. P., and Hoehn, M., Brain maturation of the adolescent rat cortex and striatum: changes in volume and myelination. Neuroimage 84:35–44, 2014.

86. Keihaninejad, S., Zhang, H., Ryan, N. S., Malone, I. B., Modat, M., Cardoso, M. J., and Ourselin, S., An unbiased longitudinal analysis framework for tracking white matter changes using diffusion tensor imaging with application to Alzheimer's disease. Neuroimage 72:153–163, 2013.

87. Sorzano, C. O. S., Vargas, J., Pascual-Montano, A. D., A survey of dimensionality reduction techniques, ArXiv, 2014.

88. Jolliffe, I. T., Principal Component Analysis. Springer Series in Statistics. New York: Springer, 2002.

89. Perlaki, G., Horvath, R., Nagy, S. A., Bogner, P., Doczi, T., Janszky, J., and Orsi, G., Comparison of accuracy between FSL's FIRST and Freesurfer for caudate nucleus and putamen segmentation. Sci. Rep. 7(1):2418, 2017.

90. Chen, H., Dou, Q., Yu, L., Qin, J., and Heng, P. A., VoxResNet: Deep voxelwise residual networks for brain segmentation from 3D MR images. Neuro Image. 170:446–455, 2018.

91. van Opbroek, A., van der Lijn, F., and de Bruijne, M., Automated brain-tissue segmentation by multi-feature SVM classification. In: Proceedings of the MICCAI Workshops—The MICCAI Grand Challenge on MR Brain Image Segmentation (MRBrainS'13), 2013.

92. Litjens, G., et al. A survey on deep learning in medical image analysis. Med. Image Anal. 42:60–88, 2017.

93. Beliveau, V., Ganz, M., Feng, L., Ozenne, B., Højgaard, L., Fisher, P., Svarer, C., Greve, D., and Knudsen, G., A High-Resolution In Vivo Atlas of the Human Brain's Serotonin System. J. Neurosci. 37(1):120–128, 2017.

94. Wang, H., Suh, J. W., Das, S. R., Pluta, J. B., Craige, C., and Yushkevich, P. A., Multi-atlas segmentation with joint label fusion. IEEE Trans. Pattern Anal. Mach. Intell. 35(3):611–623, 2013.

95. Spulber, G., Niskanen, E., MacDonald, S., Smilovici, O., Chen, K., Reimanet, E. M. et al., Whole brain atrophy rate predicts progression from MCI to Alzheimer's disease. Neurobiology of Ageing 31:1601–1605, 2010.

96. Ge, Y., Grossman, R. I., Babb, J. S., Rabin, M. L., Mannon, L. J., and Kolson, D. L., Age-Related Total Gray Matter and White Matter Changes in Normal Adult Brain. Part I: Volumetric MR Imaging Analysis. Am. J. Neuroradiol. 23(8):1327–1333, 2002.

97. Cole, J. H., and Franke, K., Predicting age using neuroimaging: innovative brain ageing biomarkers. Trends Neurosci. 40(12): 681–690, 2017.

98. Rublee, E., Rabaud, V., Konolige, K., and Bradski, G. R., ORB: An efficient alternative to SIFT or SURF. ICCV 11(1):2, 2011.

99. Lowe, D. G., Object recognition from local scale-invariant features. ICCV 99(2):1150–1157, 1999.

100. Calonder, M., Lepetit, V., Strecha, C., and Fua, P., Brief: Binary robust independent elementary features. In: European conference on computer vision, pp. 778-792, Berlin: Springer, 2010.

101. Simonyan, K., and Zisserman, A., Very deep convolutional networks for large-scale image recognition. arXiv:1409.1556, 2014.

102. Sajedi, H., Mohammadi Panah, F., and Kazemi Shariat Panah, S. H., An image analysis-aided method for redundancy reduction in differentiation of identical Actinobacterial strains. Future Microbiol 13(3):313–329, 2018.

103. Afshar, L. K., and Sajedi, H., Age Prediction based on Brain MRI Images using Extreme Learning Machine, 2019 7th Iranian Joint Congress on Fuzzy and Intelligent Systems, CFIS, 2019.

104. Pardakhti, N., and Sajedi, H., Age Prediction based on brain MRI images using Feature Learning, Subotica: SISY 2017, IEEE 15th International Symposium on Intelligent Systems and Informatics, 2017.

105. Wang, D., and Tan, X., Unsupervised feature learning with C-SVDDNet. Pattern Recogn. 60:473–485, 2016.

106. Marcus, D. S., Wang, T. H., Parker, J., Csernansky, J. G., Morris, J. C., and Buckner, R. L., Open Access Series of Imaging Studies (OASIS): Cross-Sectional MRI Data in Young, Middle Aged, Nondemented, and Demented Older Adults. J. Cogn. Neurosci. 19:1498–1507, 2007.

107. Tax, D. M., and Duin, R. P., Support Vector Data Description. Mach. Learn. 54:45–66, 2004.

108. Wu, Z., Lu, X., and Deng, Y., Image edge detection based on local dimension: A complex networks approach. Physica A: Statistical Mechanics and its Applications 440:9–18, 2015.

109. Auria, L., and Moro, R. A., Support Vector Machines (SVM) as a Technique for Solvency Analysis. Mach. Learn. 54:45–66, 2004.

110. Raji, C. A., Lopez, O. L., Kuller, L. H., Carmichael, O. T., and Becker, J. T., Age, Alzheimer disease, and brain structure. Neurology 73(22):1899–1905, 2009.

111. Mastery Farahani, R., Aliaghaei, A., Abdolmaleki, A., Abbaszadeh, H. A., Shaerzadeh, F., Norozian, M., and Moayeri, A., Sexual Dimorphism and Age-Related Variations of Corpus Callosum Using Magnetic Resonance Imaging. Anatomical Sciences 13(3):159–166, 2016.

112. Resnick, S. M., Goldszal, A. F., Davatzikos, C., Golski, S., Kraut, M. A., Metter, E. J., Bryan, R. N., and Zonderman, A. B., One-year age changes in MRI brain volumes in older adults. Cereb. Cortex 10(5):464–472, 2000.

113. Asim, Y., Raza, B., Malik, A. K., Rathore, S., Hussain, L., and Iftikhar, M. A., A multi-modal, multi-atlas-based approach for Alzheimer detection via machine learning. Int. J. Imaging Syst. Technol. 28(2):113–123, 2018.

114. Liu, M., Zhang, D., Shen, D., and Alzheimer's Disease Neuroimaging Initiative, View-centralized multi-atlas classification for Alzheimer's disease diagnosis. Hum. Brain Mapp. 36(5): 1847–1865, 2015.

115. Min, R., Wu, G., Chen, J., Wang, Q., Shen, D., and Alzheimer's Disease Neuroimaging Initiative, Multi-atlas based representations for Alzheimer's disease diagnosis. Hum. Brain Mapp. 35(10): 5052–5070, 2014.

116. Pang, S., Yu, Z., and Orgun, M. A., A novel end-to-end classifier using domain transferred deep convolution neural networks for biomedical images. Comput. Methods Prog. Biomed. 140:283–293, 2017.

117. Lu, S., Lu, Z., and Zhang, Y., Pathological brain detection based on AlexNet and transfer learning. J. Comput. Sci. 30:41–47, 2019.